


Finding balance: Tree-ring isotopes differentiate between acclimation and stress-induced imbalance in a long-term irrigation experiment

Journal Article

Author(s):

Vitali, Valentina; Schuler, Philipp; Holloway-Phillips, Meisha; D'Odorico, Petra; Guidi, Claudia; Klesse, Stefan; Lehmann, Marco M.; Meusburger, Katrin; Schaub, Marcus; Zweifel, Roman; [Gessler, Arthur](#) ; Saurer, Matthias

Publication date:

2024-03

Permanent link:

<https://doi.org/10.3929/ethz-b-000665724>

Rights / license:













[Creative Commons Attribution 4.0 International](#)

Originally published in:

Global Change Biology 30(3), <https://doi.org/10.1111/gcb.17237>

RESEARCH ARTICLE

Finding balance: Tree-ring isotopes differentiate between acclimation and stress-induced imbalance in a long-term irrigation experiment

Valentina Vitali¹  | Philipp Schuler¹  | Meisha Holloway-Phillips¹  |
 Petra D'Odorico¹  | Claudia Guidi¹  | Stefan Klesse¹  | Marco M. Lehmann¹  |
 Katrin Meusburger¹  | Marcus Schaub¹  | Roman Zweifel¹  | Arthur Gessler^{1,2}  |
 Matthias Saurer¹ 

¹Swiss Federal Institute for Forest, Snow and Landscape Research WSL, Birmensdorf, Switzerland

²Institute of Terrestrial Ecosystems, ETH Zurich, Zurich, Switzerland

Correspondence

Valentina Vitali, Swiss Federal Institute for Forest, Snow and Landscape Research WSL, Zürcherstrasse 111, Birmensdorf CH-8903, Switzerland.
 Email: valentina.vitali@wsl.ch

Funding information

Schweizerischer Nationalfonds zur Förderung der Wissenschaftlichen Forschung, Grant/Award Number: 179978, 200020_182092, 310030_189109 and 205492; HORIZON EUROPE Marie Skłodowska-Curie Actions, Grant/Award Number: 846134

Abstract

Scots pine (*Pinus sylvestris* L.) is a common European tree species, and understanding its acclimation to the rapidly changing climate through physiological, biochemical or structural adjustments is vital for predicting future growth. We investigated a long-term irrigation experiment at a naturally dry forest in Switzerland, comparing Scots pine trees that have been continuously irrigated for 17 years (*irrigated*) with those for which irrigation was interrupted after 10 years (*stop*) and non-irrigated trees (*control*), using tree growth, xylogenesis, wood anatomy, and carbon, oxygen and hydrogen stable isotope measurements in the water, sugars and cellulose of plant tissues. The dendrochronological analyses highlighted three distinct acclimation phases to the treatments: irrigated trees experienced (i) a significant growth increase in the first 4 years of treatment, (ii) high growth rates but with a declining trend in the following 8 years and finally (iii) a regression to pre-irrigation growth rates, suggesting the development of a new growth limitation (i.e. acclimation). The introduction of the stop treatment resulted in further growth reductions to below-control levels during the third phase. Irrigated trees showed longer growth periods and lower tree-ring $\delta^{13}\text{C}$ values, reflecting lower stomatal restrictions than control trees. Their strong tree-ring $\delta^{18}\text{O}$ and $\delta^2\text{H}$ (O–H) relationship reflected the hydrological signature similarly to the control. On the contrary, the stop trees had lower growth rates, conservative wood anatomical traits, and a weak O–H relationship, indicating a physiological imbalance. Tree vitality (identified by crown transparency) significantly modulated growth, wood anatomical traits and tree-ring $\delta^{13}\text{C}$, with low-vitality trees of all treatments performing similarly regardless of water availability. We thus provide quantitative indicators for assessing physiological imbalance and tree acclimation after environmental stresses. We also show that tree vitality is crucial in shaping such responses. These

Petra D'Odorico, Claudia Guidi, Stefan Klesse, Marco M. Lehmann, Katrin Meusburger, Marcus Schaub are listed in alphabetical order.

This is an open access article under the terms of the [Creative Commons Attribution](https://creativecommons.org/licenses/by/4.0/) License, which permits use, distribution and reproduction in any medium, provided the original work is properly cited.

© 2024 The Authors. *Global Change Biology* published by John Wiley & Sons Ltd.

findings are fundamental for the early assessment of ecosystem imbalances and decline under climate change.

KEYWORDS

climate change, dendroecology, deuterium, *Pinus sylvestris*, tree-ring isotopes

1 | INTRODUCTION

Climate change is driving major shifts in water availability across Europe (IPCC, 2022). These alterations have been shown to impact forests' performance and survival, challenging ecosystem resilience (Ingrisch & Bahn, 2018). Characterising the physiological acclimation potential of trees to drought is crucial (Grossiord, 2020) in order to select resilient species to stabilise forest functions under climate change (Bauhus et al., 2017). Acclimation processes (Gessler et al., 2020), defined as the physiological changes due to phenotypic plasticity which minimise the effects of stressors (Lambers et al., 1998), can provide a rapid response to altered growth conditions (Mallard et al., 2020; Nicotra et al., 2010), unlike multi-generation (evolutionary) strategies like adaptation or migration (Jump & Peñuelas, 2005; Pugnaire et al., 2019). Acclimation means trees function in a steady state; however, under stress, adjustments to the acclimation state are triggered via physiological, biochemical or structural alterations (Beaman et al., 2016; Rowland et al., 2023; Wilson & Franklin, 2002). At the onset of drought conditions, for example, physiological adjustments are made at the leaf level, including regulation of stomatal conductance to reduce water loss and avoid xylem cavitation (Gleason et al., 2016; Marchin et al., 2016) and down-regulation of Rubisco activity to balance the reduced CO₂ uptake (Parry et al., 2002). When different water availability conditions become protracted across multiple growing seasons, as in consecutive drought years or irrigation experiments, structural acclimations are triggered, such as adjustments in needle morphology and needle production (Sangüesa-Barreda et al., 2023; Timofeeva et al., 2017), changes in sapwood area (Gebhardt et al., 2023; Moreno et al., 2021) and shifts in fine-root production (Brunner et al., 2019; Joseph et al., 2020). These acclimation mechanisms further feedback on the sensitivity of stomata and photosynthetic activity (Nadal-Sala et al., 2021; Schönbeck et al., 2022), and on photochemical reflectance (D'Odorico et al., 2021), reducing the vulnerability of trees to drought conditions (Chen et al., 2022; Gessler et al., 2020), or helping them acclimate to more favourable conditions in the case of irrigation experiments (Bose et al., 2022). Organ and carbohydrate reserve turnover rates determine legacy effects (Zweifel et al., 2020), with long turnover rates prolonging acclimation responses. If the altered condition remains constant, for example, in irrigation or drought experiments, it is expected that the system will reach a new equilibrium state where water demand and supply are re-balanced (McDowell et al., 2008; Zweifel & Sterck, 2018). This is observed as a gradual dampening of the initially strong

responses connected to changes in water availability (Barbeta et al., 2013; Zweifel et al., 2020).

Research efforts to investigate the physiological and morphological legacies of unfavourable environmental conditions on trees are increasing (Anderegg et al., 2015; Bréda et al., 2006; Lindner et al., 2010). Experimental manipulations of abiotic factors in natural forests are one method to investigate acclimation processes both in the short term (i.e., daily or seasonal level; Atkin, 2003; Werner et al., 2021) and in the long term (i.e. annual, or decadal level; e.g. Martin-Stpaul et al., 2013; Pretzsch et al., 2019; Rodríguez-Calcerrada et al., 2011). However, large-scale and long-term experiments remain rare, even though they are crucial for understanding and disentangling acclimation processes in the context of the natural variability of climate and ecosystem dynamics. There are a few examples of long-term experiments in mature forests (Cotrufo et al., 2011; Loewe-Muñoz et al., 2021) where water availability has been manipulated to investigate acclimation processes, in response to reduced soil water availability by rainfall exclusion (Barbeta et al., 2013; Belluau et al., 2021; Gavinet et al., 2019; Goke & Martin, 2022; Grams et al., 2021), irrigation (Feichtinger et al., 2014; Rigling et al., 2003) or both (Beier et al., 1995). Unfortunately, such experiments seldom last longer than 10 years (Barbeta et al., 2013; Da Costa et al., 2018; Dobbertin et al., 2010; Feichtinger et al., 2014; van Sundert et al., 2023), despite the fact that it is becoming apparent that acclimation processes might take longer (Bose et al., 2022). Here, we investigate these processes in the 17-year long irrigation experiment set in the Pfywald forest in Switzerland using a multi-proxy approach.

Combining different proxies of tree growth and functioning makes it possible to study the dynamics of acclimation processes (Table 1), and to retrospectively quantify seasonal changes in needle tissues and wood traits and decadal changes in growth dynamics (Rowland et al., 2023). Quantitative wood anatomy provides insights into wood formation processes (Fonti et al., 2010) and adaptations of xylem structures (Prendin et al., 2017; von Arx & Carrer, 2014). For example, the production of smaller xylem conduits in response to drought has been associated with improved drought tolerance (Fonti et al., 2010; Zimmermann et al., 2021). Conversely, the release from drought through irrigation may be associated with an increase in xylem conduit size or mean hydraulic diameter, allowing higher rates of transpiration and growth (Anfodillo & Olson, 2021). Differences in the timing of events can be connected to water availability regimes by tracking wood formation throughout the growing season (i.e. xylem creation

TABLE 1 Tree-ring width (TRW), quantitative wood anatomy (QWA), isotopes measured in tree tissues and tree-ring cellulose ($\delta^{13}\text{C}$), and changes in the relationship between $\delta^{18}\text{O}$ and $\delta^2\text{H}$ (O–H relationship) are proxies used to quantify the physiological and structural acclimation responses of trees to altered environmental conditions, providing an overview of tree functioning.

Proxy	TRW	QWA	$\delta^{13}\text{C}$	O–H relationship
Inferred variables	Climate	Water transport	Photosynthetic activity	Hydrological signature
	Carbon allocation	Timing of cell formation	Stomatal conductance	Metabolic impact
Tree functioning	Growth	Hydraulic capacity	Canopy functioning	Acclimation status

and carbon allocation), due to the high sensitivity of cell division and enlargement to both cell turgor and sugar availability (Caban et al., 2020; Fatichi et al., 2014; Körner, 2015).

Isotopes in tree-ring cellulose are a proxy used to infer the physiological processes that occur during tree-ring cellulose formation and thus a tree's response to environmental conditions. To understand the physiological signals recorded in the isotopes of tree-ring cellulose, we need to disentangle the processes that cause isotope fractionation, that is, a physiological process can only be recorded if isotope fractionation is involved. ^{13}C -fractionation is related to assimilation rate and stomatal conductance (Frank et al., 2015; Saurer et al., 2014), whereas transpiration causes evaporative ^{18}O and ^2H -enrichment, which is incorporated into sugars with associated equilibrium isotope effects (Craig & Gordon, 1965; Dongmann et al., 1974; Farquhar et al., 2007). However, fractionations during assimilate transport (e.g. Gessler et al., 2004) and metabolic processes (Kagawa & Battipaglia, 2022; Wieloch et al., 2022; Yakir & DeNiro, 1990), including both kinetic and equilibrium isotope exchange with xylem water, resulting in a dampening of the initial leaf-level hydrological signal. Importantly, the metabolic-associated isotope effects are different for O and H (Hayes, 2001; Holloway-Phillips et al., 2022), leading to differential isotope patterns in cellulose (Holloway-Phillips et al., 2023). Carbon ($\delta^{13}\text{C}$) and oxygen ($\delta^{18}\text{O}$) isotopic ratios in tree rings have been used extensively as proxies for canopy functioning (Farquhar et al., 1982; Scheidegger et al., 2000; Vitali et al., 2021), and to investigate past climatic conditions (e.g. Andreu-Hayles et al., 2017; Loader et al., 2007; Saurer et al., 1997) and tree physiological performance (e.g. Frank et al., 2015; Guerrieri et al., 2019; Levesque et al., 2019). Meanwhile, $\delta^2\text{H}$, which has been studied far less, appears to record a mixture of the climate signal (i.e. the hydrological signal derived from the source water, precipitation and atmospheric exchange) and a physiological or metabolic signal dependent on carbon metabolism during photosynthesis and post-photosynthesis, as well as differential C-resource use (Terwilliger & Deniro, 1995; Vitali et al., 2023; Yakir & DeNiro, 1990).

$\delta^{18}\text{O}$ and $\delta^2\text{H}$ have often been assumed to have a strong positive relationship inherited from the source water (Dansgaard, 1964). However, isotope fractionations during the biosynthesis of organic compounds (heron metabolic share of the isotope signals) are not coupled for $\delta^{18}\text{O}$ and $\delta^2\text{H}$ (Holloway-Phillips et al., 2022, 2023). As a result, the relationship between $\delta^{18}\text{O}$ and $\delta^2\text{H}$ (hereafter O–H relationship) is weaker than expected if it were based only on the hydrological signal and was shown to be dependent on site conditions and

year-to-year variation (Nabeshima et al., 2018; Vitali et al., 2022). In natural settings, in the event of extreme defoliation by larch budmoth outbreaks (*Zeiraphera griseana* [Hübner]; Vitali et al., 2023), the O–H relationship has been found to be significantly weaker than in non-defoliated years. This was suggested to reflect the utilisation of carbon reserves for the formation of wood and canopy re-flushing, due to the lower availability of fresh assimilates (Kimak, 2015; Nabeshima et al., 2018; Sanchez-Bragado et al., 2019). Thus, in defoliated years the share of isotope signal connected to the metabolic processes modifies the O–H relationship masking the 'normally' recorded hydrological signature (Vitali et al., 2023). By extension, we hypothesise that in non-perturbed growing conditions, where we assume that trees function in physiological balance or an acclimated state, the hydrological isotope signature is more strongly imprinted in the tree-ring cellulose. In the event of perturbations (e.g. substantial and sustained shift in the water balance), the metabolic signal induces a decoupling of the O–H relationship indicating a physiological imbalance (conceptualised in Section 4.4).

Our main aim was to investigate the response of Scots pine (*Pinus sylvestris* L.) to changes in water availability, in the Pfywald irrigation experiment to evaluate its capacity to acclimate to new growing conditions by structural changes and adapting its physiological functioning. By analysing multiple proxies, we retrospectively inferred the growth (tree-ring width, TRW), hydraulic capacity (QWA), photosynthetic and transpiration conditions of the canopy ($\delta^{13}\text{C}$), and acclimation state (O–H relationship, Table 1) of trees under different water availability regimes. Specifically, we investigated two treatments: (i) 17-year irrigation doubling rainfall amounts during the vegetative period (irrigation) and (ii) 11 years of irrigation followed by 6 years of non-irrigated conditions (stop). We compared these treatments with exclusively rainfed controls. We also assessed differences between trees that differed in crown transparency (see Dobbertin et al., 2004), as a proxy for tree 'vitality' (with high vitality defined as good growth and low crown transparency), as this property has been shown to play a role in trees' photosynthetic performance (Eilmann et al., 2013; Schönbeck et al., 2018). We hypothesised that:

Hp 1. Long-term structural and physiological acclimation responses would indicate that:

- trees have reached a new growth equilibrium under irrigation and
- the stop treatment has induced a new stress condition triggering new acclimation processes.

Hp 2. The responses to treatments and acclimation processes would depend on tree vitality.

Hp 3. The O–H relationship of stable isotopes in tree rings can be used as a proxy for the extent of forests' acclimation to altered environmental conditions.

2 | MATERIALS AND METHODS

2.1 | Experimental setup and sample selection

The Pfywald irrigation experiment is located in a Scots pine forest in southwestern Switzerland that is more than 100 years old (46°18'N, 7°36' E, 615 m a.s.l.). The dry inner-Alpine valley of the Rhone River has a mean annual temperature of 10.1°C and an annual precipitation of 600 mm (Houston Durrant et al., 2016), with a considerable dry period during the summer months; it can be considered the dry edge of the natural distribution of Scots pine. The soil is characterised by low water retention (Brunner et al., 2009). The experimental setup divides a portion of the Pfywald forest (1.2 ha; ~800 trees) into eight plots of 25 × 40 m each, separated by 5-m-wide buffer zones (Figure S1). The irrigation treatment, started in 2003, doubles the natural annual precipitation. From May to October, night irrigation by sprinklers at 1-m height distributes ~600 mm/year, using water from a nearby channel. In 2014, the irrigation treatment was halted in half of the area of the irrigated plots. This resulted in three water regimes: four control plots (C) that have never been irrigated and correspond to the natural dry conditions; four irrigated plot areas (I) that have been irrigated each year since 2003, experiencing a release from soil drought; and four irrigation-stop plots areas (S) that have not been irrigated since 2014.

In this study, measurements were carried out in 2019, using eight Scots pine trees per treatment (Figure S1). Crown transparency has been monitored every year in Pfywald (Figure S2), and according to the findings of Dobbertin et al. (2004) and Schönbeck et al. (2018) has been observed to be a key proxy for trees' photosynthetic performance. Thus, the sampling strategy was stratified: for each treatment, four trees with low crown transparency in 2019 (<20%, hereafter H for high-vitality) and four trees with high crown transparency in 2018 (>40%, hereafter L for low-vitality) were selected. Four sampling campaigns were performed throughout the 2019 vegetative season, on 4 June (after the initial needle flush), 15 July, 25 August and 20 October (when the 2019 tree ring was completely formed). On each sampling date, micro-cores (2-mm diameter, 15-mm length) were collected with a standard puncher kit and stored in a 96% water–alcohol solution until xylogensis analyses. Additionally, in the October campaign, two 5-mm increment cores were extracted at breast height (1.30 m) from each tree with an increment borer (HAGLÖF; Långsele, Sweden).

For all target trees, samples from the current-year needles (Ne), twig xylem (Tx), twig phloem (Tp), and stem xylem (Sx) and

phloem (Sp) were collected in exetainers (Exetainer glass vials, Labco, Lampeter, Wales, UK, prod. No. 738W) and stored in dry ice. Branches were cut from the fully light-exposed portion of the crown with an extendable pruner. Next to each target tree location, soil samples were collected at a 10–20 cm depth, which has been found to be the main depth where trees take up water at this site (Timofeeva et al., 2020) and the root material was sieved out.

Increment cores were processed following standard dendro-chronological procedures (Cook & Kairiukstis, 1990). TRWs were measured at 0.01-mm precision and cross-dating validated followed standard procedures (Bunn, 2010; Holmes, 1983).

2.2 | Water, cellulose and sugar extraction from plant tissues

2.2.1 | Water

Water was extracted from all sampled tissues (i.e. needles, branch and stem xylem and phloem, and soil), by cryogenic vacuum distillation (Diao et al., 2022; West et al., 2006). In short, all samples were heated at 80°C in a water bath for 2 h to ensure complete extraction and the vapour was collected by glass traps submerged in liquid nitrogen.

2.2.2 | Cellulose

Dated annual tree rings were hand-cut and separated for 2000–2019, and earlywood and latewood were separated for 2019 alone. Tree ring, twig and needle cellulose were extracted using F57 fibre filter bags (Ankom Technology, Macedon, NY, USA) and standard purification methods (Boettger et al., 2007). Cellulose from all tissues was homogenised and packed into silver capsules for the measurement of $\delta^{13}\text{C}$, $\delta^{18}\text{O}$ and $\delta^2\text{H}$.

2.2.3 | Sugars

Following the cryogenic vacuum distillation, dry needles and phloem tissues were ball-milled (MM400, Retsch, Haan, Germany), and sugars were extracted from 100 mg of needle powder and phloem powder following established protocols (Lehmann et al., 2020; Rinne et al., 2012). Briefly, the ground material was mixed with 2 mL of deionised water and heated to 85°C for 30 min to extract the water-soluble content. The sugar fraction of the water-soluble content was then purified using ion exchange cartridges (OnGuard II A, H and P, Dionex, Thermo Fisher Scientific, Bremen, Germany). The purified sugar solutions were frozen and freeze-dried, and then packed into silver capsules for stable isotope measurements.

2.3 | Stable isotope measurements

2.3.1 | Water

The $\delta^{18}\text{O}$ and $\delta^2\text{H}$ ratios (expressed in per mil [‰] notation relative to V-SMOW [Vienna Standard Mean Ocean Water]) of the extracted water were analysed using a pyrolysis-IRMS (isotope ratio mass spectrometer) connected to a Delta Plus XP IRMS via a ConFlo III interface (Thermo Fisher Scientific, Bremen, Germany). The long-term instrument precision, measured using independent quality control standards, is 2‰ for ^2H and 0.2‰ for ^{18}O (Diao et al., 2022).

2.3.2 | Cellulose and sugars

$\delta^{13}\text{C}$ and $\delta^{18}\text{O}$ were measured by combustion in an elemental analyser using a high-temperature pyrolysis system (TC/EA) coupled to an isotope ratio mass spectrometer (IRMS, Delta Plus XP), with a precision of ca. $\pm 0.1\%$ for $\delta^{13}\text{C}$ and $\pm 0.3\%$ for $\delta^{18}\text{O}$ (Weigt et al., 2015). Corrections for past changes in the $\delta^{13}\text{C}$ of atmospheric CO_2 were applied to the raw $\delta^{13}\text{C}$ data (Leuenberger, 2007). For measuring non-exchangeable C-bound $\delta^2\text{H}$, the cellulose and sugar samples were equilibrated with the hot-water-vapour equilibration method described by Schuler et al. (2022), to correct for the O-bound H isotopes (which readily exchange with water vapour) in cellulose and to determine the non-exchangeable C-bound $\delta^2\text{H}$, with a precision of 2‰–4‰. In brief, samples were packed into silver capsules, equilibrated at 130°C with water of known isotopic composition for 2h, and dried with dry nitrogen gas for 2h. The samples were then transferred to a heated autosampler (80°C) of a high-temperature pyrolysis system (PYROcube, Elementar, Hanau, Germany). The shielded autosampler was flushed with argon, and the samples were kept there for 2h to stabilise in this environment. The samples were then thermally decomposed at 1420°C, and the isotopic ratios of H were measured by mass spectrometry (Loader et al., 2015; Weigt et al., 2015).

2.4 | Wood anatomy

The collected microcores were embedded in paraffin and cut into 7- μm -thick transverse sections using a rotary microtome (RM2245, Leica Biosystems, Nussloch, Germany). The sections were stained (with safranin and astra blue to differentiate cellulose and lignin) and mounted on glass slides. Digital images were taken for the visible rings for each slide using a slide scanner (Axio Scan Z1; Zeiss, Oberkochen, Germany).

Cell measurements were performed on the microsections under visible and polarised light to distinguish the distinct phases of cell development (Rossi et al., 2006). Cells in the cambial, enlargement, cell-wall-thickening and mature phases were visually discriminated and counted for each sample according to Cuny

et al. (2019). The ROXAS software for semi-automated cell analysis (von Arx & Carrer, 2014), combined with Image-Pro Plus (Media Cybernetics, Rockville, MD, USA), was used to measure tracheid properties for the visible rings. For the Years 2017, 2018 and 2019, the mean hydraulic diameter of the cells (Dh; Kolb & Sperry, 1999) was measured with respect to the cells' positional information through tracheidograms using the RAPTOR package (Peters et al., 2018) in R (R Core Team, 2022).

2.5 | Quantification of treatment effects and identification of acclimation phases

The responses of the trees to the irrigation treatment have not been constant as the experiment has progressed, and in previous studies, the acclimation speed has been shown to differ among tissues (Zweifel et al., 2020; Zweifel & Sterck, 2018). Here, three distinct phases were identified in the measured tree-ring chronologies by their significantly different TRW averages (Figures S3 and S4), and changes in growth trends (Figure S5), which were thus defined as: phase 1: 2003–2006; phase 2: 2007–2013; and phase 3: 2014–2019 (Figure S3; Section 3.1). To investigate the effect of the treatments, the response variables were set relative to the mean values of the high-vitality group of the control trees (CH), hereafter referred to as 'normalisation'. Groups are defined by their treatment (C=control, I=irrigated, S=Stop) and vitality (H=high and L=low) respectively resulting in the following groups: CH, CL, IH, IL, SH and SL. This normalisation was performed at the annual level for the tree-ring-based samples and by sampling campaign for the samples collected in 2019. TRWs were first log-transformed, and all normalisations were performed via subtraction (TRW_{norm} , $\delta^n X_{\text{norm}}$). Repeated measures analysis of variance (ANOVA; $p < .05$) and Tukey's honestly significant difference (HSD) post hoc tests were conducted to compare differences in the vitality levels and acclimation phases. Linear models were used to evaluate trends in the variables.

3 | RESULTS

3.1 | Acclimation phases and impact of long-term irrigation on tree biomass

The normalised TRW chronologies (TRW_{norm}) showed significant changes in growth levels (Figure 1b; Figure S3) during the 17 years of the Pfywald irrigation experiment. Three distinct growth phases could be identified: (1) increasing growth rates, (2) decreasing growth rates and (3) drop to control level (in I trees) and even lower growth rates (in S trees).

Phase 1 was restricted to the Years 2003–2006, where growth increments (TRW_{norm}) of the irrigated trees showed a significant increase from pre-irrigation growth (Figure 1b; Figure S3), reaching its maximum in 2006. In this phase, irrigated tree growth increased by

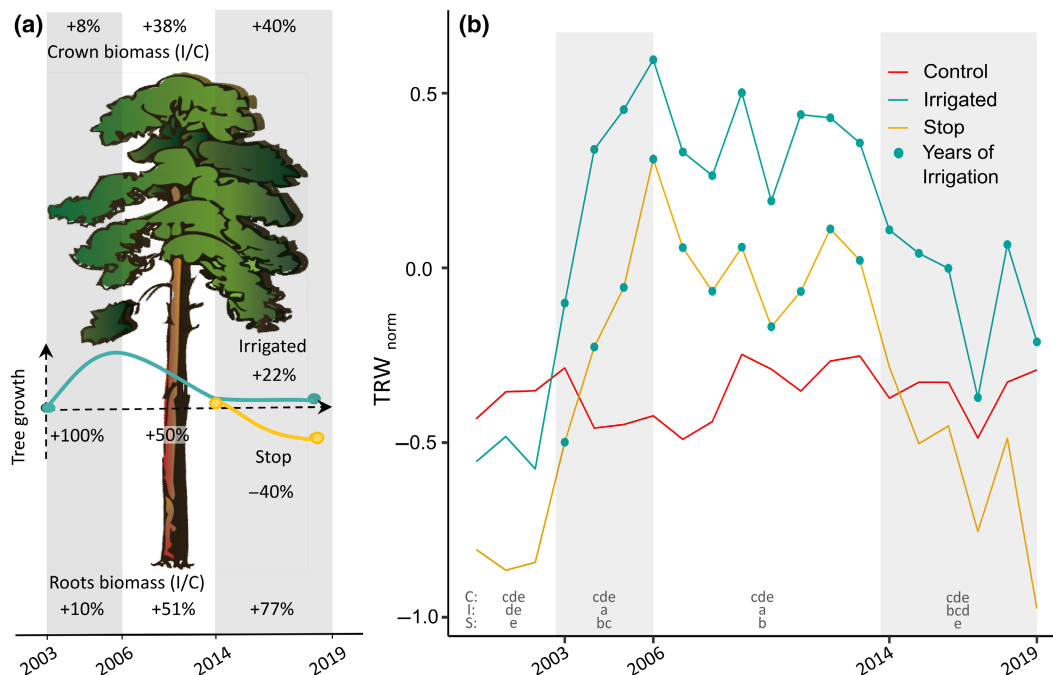


FIGURE 1 (a) Identification of the three acclimation phases of Scots pine (*Pinus sylvestris*) trees in the Pfywald experimental site, for the irrigated (I), stop (S) and control (C) treatments. Irrigation started in 2003 and ended in 2014 in the stop treatment (indicated by the blue dots). The percent changes in crown and root biomass are calculated for the irrigated trees relative to the control trees for different periods, where crown biomass increment rates are based on leaf area index (LAI) from Bose et al. (2022); and stem growth and root biomass are taken from Brunner et al. (2019) and Guidi et al. (unpublished). Stem percentual changes are calculated from all trees' tree-ring width chronologies relative to control until 2014, and for irrigated and stop trees separately after 2014. (b) Average normalised tree-ring-width chronologies (TRW_{norm}) and their statistical differences between the treatments for the acclimation phases (ANOVA; post hoc test, $p < .05$, indicated by different lowercase letters). In both panels (a) and (b), the three acclimation phases, showing significantly different growth patterns (see Figure S3), are distinguished with grey shading (i.e. phase 1: 2003–2006; phase 2: 2007–2013; phase 3: 2014–2019).

100% relative to control trees, meeting the new growth potential set by the increased water availability (Figure 1a). This radial growth increase was matched by gradual increases in biomass relative to the control trees, reaching +8% in the crown (based on leaf area index (LAI) measurements from Bose et al., 2022) and +10% in the fine roots by 2006 (Brunner et al., 2019).

The beginning of **phase 2** was identified by a decrease in growth rates. In phase 2 (2007–2013), the TRW_{norm} of all irrigated trees was still significantly greater (50%) than that of the control trees. On average, crown and root biomass were significantly greater in irrigated trees (+38% and +51%, respectively, Figure 1a).

Phase 3 was characterised by significantly reduced TRW_{norm} than phase 2, with irrigated trees almost returning to pre-irrigation growth rates (i.e. before 2003), but also converging with the growth rates of the control trees (Figure 1b). Irrigated trees still had a 22% greater TRW_{norm} than control trees (Figure 1; Figure S3), but due to the declining trend, this difference was not statistically significant, indicating a clear dampening of the irrigation effect. Contrarily, both crown and fine root biomass were still elevated in the irrigated trees in phase 3 (+40% and +77%, respectively; Figure 1a). The beginning of phase 3 corresponded to the interruption of the irrigation for the stop trees in 2014, which resulted in an average growth reduction of -40%, reaching rates below the control and similar to pre-irrigation levels (Figure 1).

3.2 | Impact of tree vitality level on tree growth and tree-ring isotopic signature

Significant differences were observed between the two canopy vitality levels in both the TRW and the tree-ring isotope chronologies. The high-vitality trees (H) showed significantly higher growth rates (TRW) than the low-vitality trees (L), regardless of the treatment (Figure 2a). The TRW patterns of the irrigated trees showed similar trends for the two vitality levels (Figure S5). On the contrary, the growth of the SH trees showed a much larger decrease than that of the SL trees in phase 3 (Figure 3). To specifically investigate the impact of the removal of irrigation in 2014, we normalised the chronologies to the IH trees, as both treatments were equally irrigated in the Years 2003–2014 (Figure 3). Stopping irrigation triggered a gradual but statistically significant growth reduction of -40% in stop trees in the years following 2014, with the most dramatic decline in growth for the SH trees. By 2015 the SL and SH trees grew at similar levels. The growth rate of the SL trees overlapped that of the IL trees, indicating that vitality level strongly drove growth patterns independently of water availability.

The acclimation phases identified from the TRW averages (Figure 1) were also reflected in changes in the annually resolved isotope ratio chronologies ($\delta^{13}C$, $\delta^{18}O$ and δ^2H ; Figure 2; Figures S4 and S5). In all acclimation phases, both irrigated and stop trees had, on average, lower $\delta^{13}C$ values than control trees,

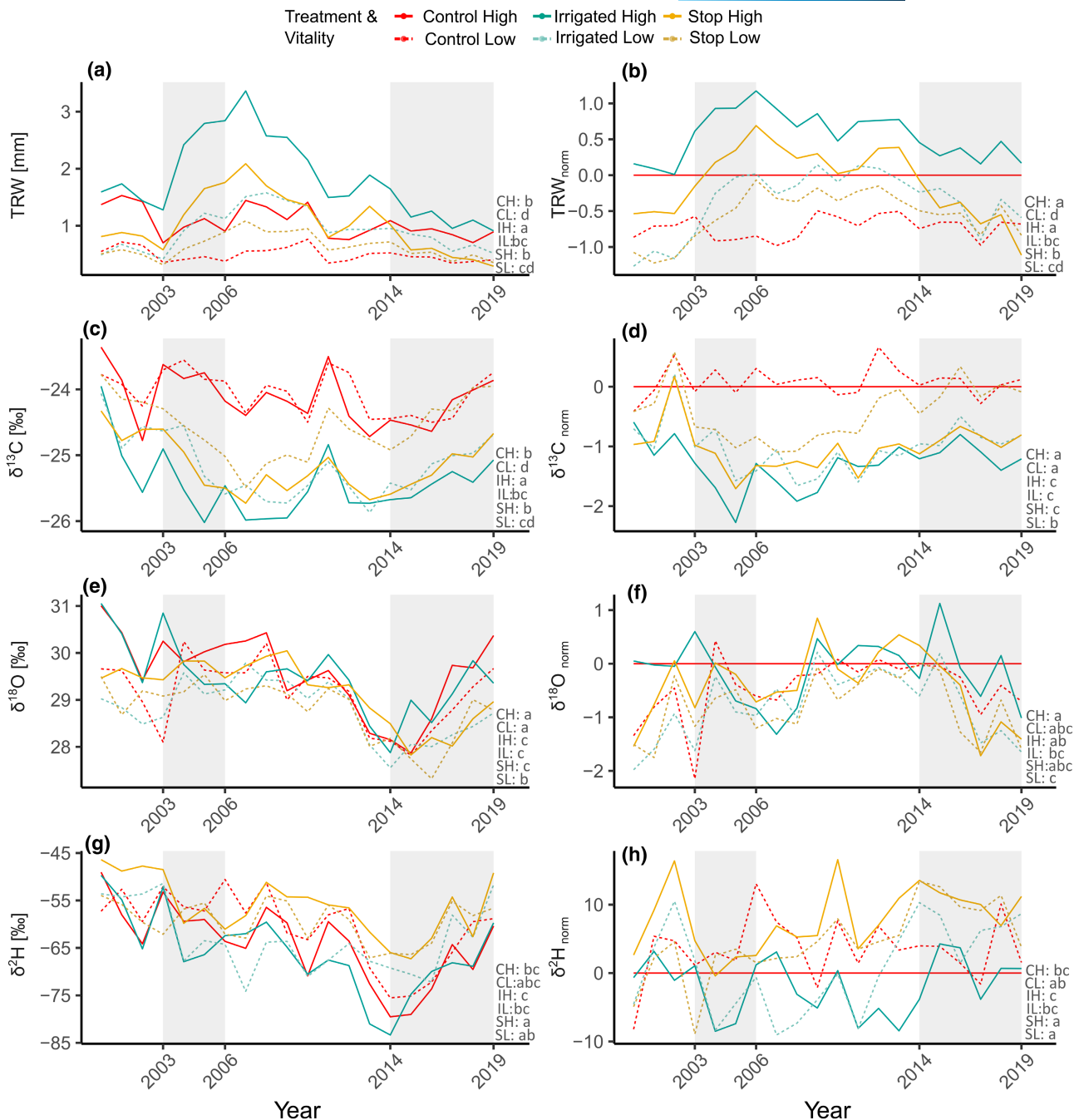


FIGURE 2 Average chronologies of tree-ring width (TRW; a) and tree-ring isotope ratios for $\delta^{13}\text{C}$ (c), $\delta^{18}\text{O}$ (e) and $\delta^2\text{H}$ (g) for the two vitality levels (low, high) and three treatments (control, irrigated and stop). The different acclimation phases (phase 1: 2003–2006; phase 2: 2006–2014; phase 3: 2014–2019) are indicated with grey shading. The right panels (b, d, f, h) show the TRW_{norm} chronologies. Statistical differences between the treatments for the different vitality levels are shown for the whole experimental period (i.e. 2003–2019, analysis of variance and post hoc tests, $p < .05$, indicated by lower case letters). See Figure S4 for statistical differences between treatments and vitalities in the three phases and Figure S5 for a decomposition of the slopes.

and the high-vitality trees had lower $\delta^{13}\text{C}$ values than the low-vitality ones, regardless of the treatment (Figure 2c,d). The overall trends were common for all treatments and vitality levels, with the increase in water availability initially inducing a significant decrease of the $\delta^{13}\text{C}$ ratios, followed by a gradual increasing trend in the second and third phases. However, the stop treatment showed the strongest difference between the two vitality

levels, which started diverging in phase 2. The $\delta^{13}\text{C}$ chronologies of the SH trees followed the pattern of irrigated trees and did not go back to control levels even after years of no irrigation, while the SL trees showed consistently higher $\delta^{13}\text{C}$ values, similar to those of the control trees, throughout all three phases.

During the experimental period, the $\delta^{18}\text{O}$ (Figure 2e,f) and $\delta^2\text{H}$ (Figure 2g,h) isotope chronologies of the treatments showed similar

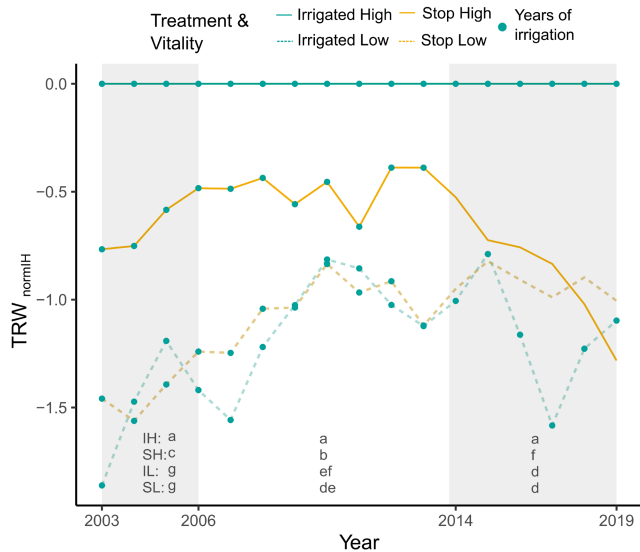


FIGURE 3 Tree-ring chronologies of the two vitality levels (low, high) of the stop and irrigated trees normalised to the mean of the irrigated high-vitality trees (TRW_{normIH}). Blue dots indicate years when the trees were irrigated, and grey shading indicates the three acclimation phases. Comparisons between and within groups and time periods were carried out with a multi-factor analysis of variance and post hoc tests ($p < .05$ indicated by lower case letters).

trends, with an initial gradual decline reaching a minimum in 2014, and a gradual increase thereafter. The $\delta^{18}O_{norm}$ chronologies of low-vitality trees (Figure 2e) showed a 1‰ lower $\delta^{18}O$ for the first 4 years of treatment (phase 1). These vitality-dependent differences disappeared between 2009 and 2014 (phase 2), only to emerge again in 2014, with IL values decreasing significantly. Meanwhile, the IH trees oscillated around the CH values. The $\delta^{18}O$ chronologies of the irrigation and the stop treatments matched during the first two phases, to be expected given the shared source water, while in phase 3 the SH, SL and IL chronologies became increasingly more depleted in ^{18}O than the IH trees (Figure 2e; Figures S4 and S5).

δ^2H values show higher year-to-year variability than the other isotopic ratios throughout the experimental period (Figure 2g,h), albeit with a similar shape as the $\delta^{18}O$ chronology. The irrigated and stop treatments diverged from the control in opposite directions, with irrigated trees on average having δ^2H values 5‰ lower than that of CH trees, and the stop trees having values ~5‰ higher. δ^2H increased significantly for SH and SL trees in phase 2, and increased significantly for IH and IL trees in phase 3 (Figure S4). No significant differences between vitality levels were observed, besides between IH and IL in phase 3 (Figure S4).

3.3 | Impacts of tree vitality on wood formation and functioning

During the vegetative season of 2019, the irrigated trees produced a similar number of cells compared with control trees, while the stop trees produced significantly fewer cells. Vitality level had the largest influence on the number of cells produced in the irrigated trees (on average,

IH=31 cells, IL=17 cells) and control trees (CH=28 cells, CL=13 cells), while there were no differences in the stop treatment (SH and SL=11 cells). The timing of carbon fixation in the tree rings differed significantly between treatments and also between vitality levels. CH and IH trees were active throughout the vegetative season, with a significant increase in the number of mature cells (i.e. cells where secondary cell walls are fully lignified) both between the first and second sampling dates (June to July) and between the third and fourth dates (August to October, Figure 4b). A large amount of enlarging and thickening of the cells had occurred by the third sampling date (Figure S6). On the contrary, stop trees and all low-vitality trees had completed most of their cell maturation by July, regardless of the treatment, as no new mature cells were detected between the third and fourth sampling dates.

The overall mean hydraulic diameter (D_h ; Kolb & Sperry, 1999) showed distinct differences between the two vitality levels in all treatments, with a strong difference for the irrigated trees (Figure 5). The IL trees had much lower $D_{h_{norm}}$ values than the CL and SL trees. At the beginning of the vegetative season the maximum value of D_h was similar for all treatments, but the $D_{h_{norm}}$ of IH trees increased in the middle of the ring, while the values strongly declined for IL trees. Stop trees with both vitality levels had lower $D_{h_{norm}}$ values than the control.

3.4 | Impact of irrigation treatments on isotope variation in tree tissues in 2019

We traced the isotopic variation from samples of water to the organic compounds in the trees, following the water uptake and assimilation path (Figure 6g). The measurements of these tissues from the four sampling campaigns revealed seasonal variation in water and sugar isotopic composition, but the variation between the treatments remained constant throughout the vegetative season (see Figures S6–S12 for seasonal compound-specific variation). Therefore, we focused on the annual average patterns of isotopic composition and on the changes in relation to the CH trees ($\delta^N X_{norm}$, Figure 6c,d,f).

Irrigated trees (IH, IL) had significantly lower $\delta^{13}C$ values in sugars, with an average of -2‰ compared with CH (Figure 6a,b). On the contrary, the stop trees showed a mixed response, with $\delta^{13}C$ values consistently more similar to the control trees in sugars and in needle and twig cellulose, but more similar to the irrigated trees in wood cellulose.

In irrigated trees, ^{18}O was depleted (-2.5‰ $\delta^{18}O$) in the water of all tissues. This finding was expected, as the water used for irrigation was sourced from a nearby channel with a (depleted) isotopic signature of -13‰ $\delta^{18}O$ and -133‰ δ^2H . However, this signature was diluted from the soil to the xylem water and varied during the season (Figures S7 and S8). We observed further overwriting of this depleted source water signal during the formation of the organic matter, where the difference was smaller than 1‰ (Figure 6c,d). Trees with the stop treatment had water isotopic values similar to those of the control, since no irrigation had occurred since 2014. However, the needle sugars showed a

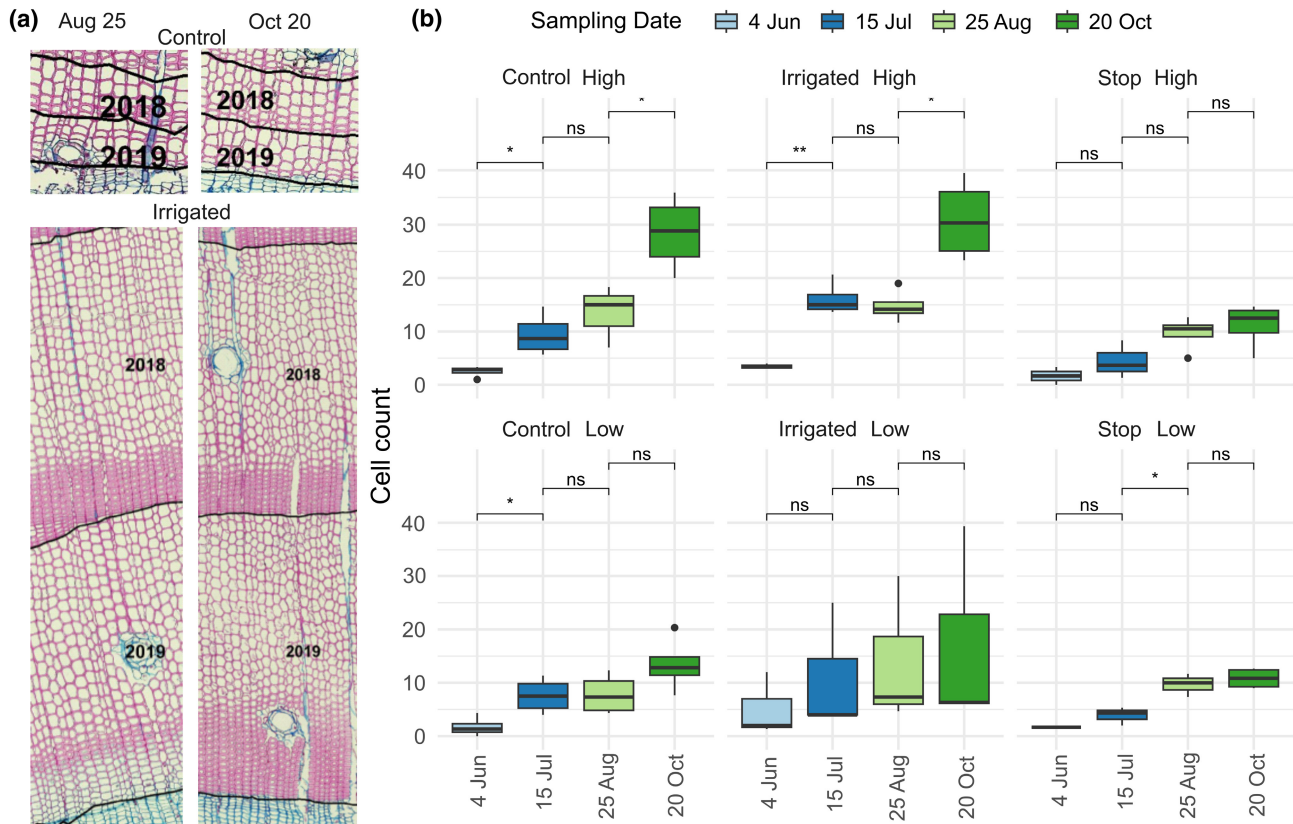


FIGURE 4 (a) Wood anatomical photos of the two extremes: low-vitality control (CL) and high-vitality irrigated (IH) trees for the Years 2018 and 2019, highlighting the ongoing cell formation in irrigated trees in August, compared to the fully completed ring in the control. (b) Normalised measurements of cell count of mature cells for the different treatments and vitality levels on the four sampling dates (4 June, 15 July, 25 August and 20 October). Significant differences between groups are indicated by asterisks ($p \geq .05$ = not significant (ns); $p < .05$ = *; $p < .01$ = **).

strong ^{18}O -depletion, reaching levels similar to those of the irrigated trees, and EW and LW showed an even stronger depletion than the irrigated trees (-3%).

The $\delta^2\text{H}$ of water samples of irrigated trees showed the expected ^2H -depletion (-10% $\delta^2\text{H}$), but the sugars showed a strong ^2H -enrichment. In particular, the $\delta^2\text{H}$ of the needle sugar of IH trees showed a 20% ^2H -enrichment compared with all other treatments. However, this enrichment was lost in the cellulose samples, where values returned to the same range as the stop ($\pm 10\%$) and control trees (Figure 6e,f).

3.5 | O-H relationship

The O-H relationship degraded along the metabolic pathway from water to cellulose. Xylem water and needle water showed a strong O-H relationship, with similar slopes between the treatments and vitality levels (Figure 7a), with an average slope of $a = -6$ for xylem water and an R^2 of 0.88. Both needle water and needle sugars showed increased variability between treatments and lower values for slope and R^2 ($a = -2$, $R^2 = \sim 0.35$ for needle water; $a = -4.5$, $R^2 = \sim 0.35$ for needle sugars), as expected due to evaporative enrichment.

Tree-ring cellulose showed the weakest O-H relationship along the metabolic pathway, with a further drop in R^2 (Figure 7d). The pairs CH-IH ($a = 6.25/6.71$) and CL-IL ($a = 6.93/6.35$) showed similar trends, with slopes close to that of xylem water, although R^2 remained lower (-0.1 - 0.2 ; Figure 7d). The tree-ring cellulose of the stop trees showed the least steep O-H relationship in the tree-ring cellulose (SH $a = 4.02$; SL $a = 1.61$). As water and sugar samples were collected at different times of the day for each tree, the impact of temperature on the water and sugars in the tree needles was analysed (Figure S14). Temperature response curves showed a stronger ^{18}O - and ^2H -enrichment for the control and stop trees. $\delta^{18}\text{O}$ and $\delta^2\text{H}$ for needle sugars both tended to decrease as temperatures increased.

4 | DISCUSSION

4.1 | Irrigation treatment and a new equilibrium state

Distinct acclimation phases were identified by significant changes in the wood growth patterns of irrigated trees relative to control trees, with an initial increase in wood growth for the first 5 years

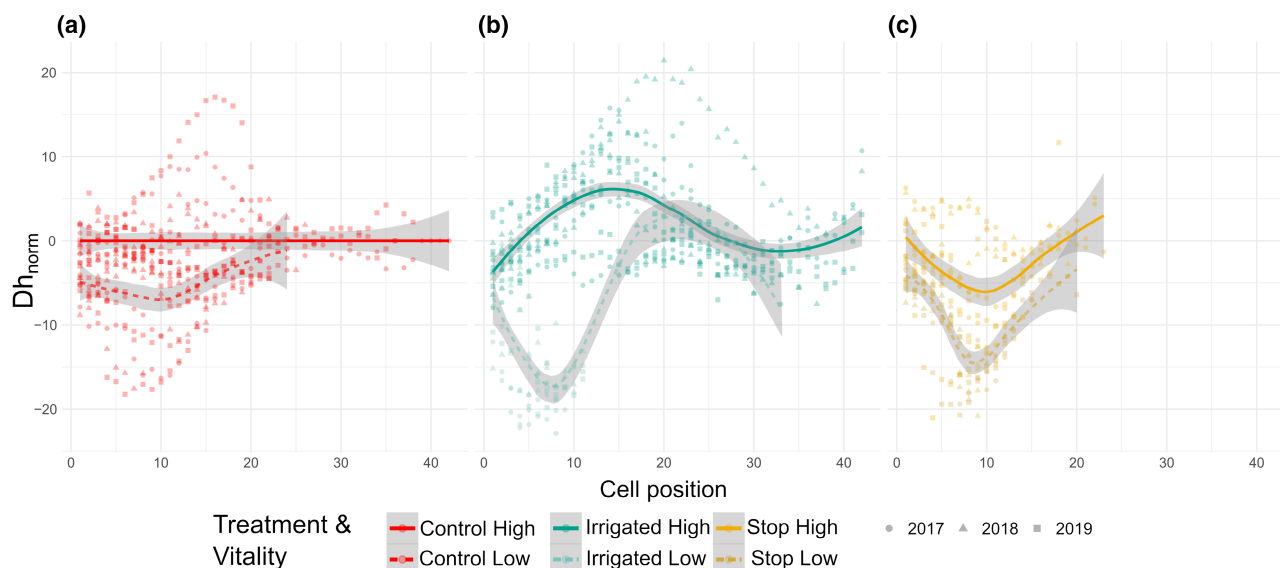


FIGURE 5 Mean hydraulic diameter (Dh_{norm}) normalised to the high-vitality control trees (CH) for the Years 2017, 2018 and 2019 for the three treatments (a) control, (b) irrigated and (c) stop; and the two vitality levels according to the recorded cell position, from 0 (beginning of earlywood, EW) to the last measured cell in the latewood (LW).

of irrigation, followed by a gradual decline (Figure 1). After 11 years of irrigation, the positive effect of increased water availability with the irrigated treatment was dampened, and we observed a stabilisation of the growth trends and a convergence to pre-irrigation growth levels. This supports our hypothesis that a new equilibrium growth state was achieved, where the increased biomass has acclimated to the surplus of water availability from the irrigation, thus reaching the new carrying capacity of the ecosystem (Hp1a). Retrospectively, we can define the initial increase in growth as a temporary overyielding, as it was not sustained in the long term (Barbata et al., 2013; Dobbertin et al., 2010).

The irrigation effects were visible not only in growth but also in cambial activity, and were modulated by tree vitality. Irrigation increased cambial activity (i.e. total number of cells); however, CH and IH trees showed similar cell production timing (Figure 4b). This did not proceed linearly within the annual ring but rather involved a larger number of cells maturing in late summer (August and September), than in mid-summer (June and July), likely due to limited water availability (Eilmann et al., 2011; Soudant et al., 2016). As we hypothesised (Hp2), the variation in xylem cell production was greater between vitality levels than between treatments, as observed previously by Eilmann et al. (2013). Both CH and IH trees showed longer cambial activity, and more cells produced and matured, during late summer compared with low-vitality trees, as well as protracted cell maturation until autumn, despite being under different water regimes. The hydraulic diameter (Dh) was also more similar within vitality levels than within treatments (Hp2), suggesting that xylem anatomical adjustments are proportional to tree canopy size, with hydraulic efficiency prioritised over safety (Prendin et al., 2018), especially for the high-vitality trees. In fact, only in high-vitality trees did we observe the expected increase in conduit size in the irrigated trees connected

to the release from limited water availability (Fonti et al., 2010; Zimmermann et al., 2021). Furthermore, low-vitality trees had systematically smaller Dh values in the earlywood, pointing to decreased osmotic potential and turgor pressure, and thus less cell enlargement (Jyske & Hölttä, 2015; Klesse et al., 2021; Peters et al., 2021). Thus, the low-vitality trees did not benefit from increased water availability as much as the high-vitality trees and maintained a more conservative strategy. Over several decades, a conservative strategy may lead to weakening and higher mortality risk (Timofeeva et al., 2017).

The different acclimation phases were also reflected by the ratios of isotopes in the tree rings. Higher water availability induced a significant ^{13}C -depletion in the irrigated trees, suggesting overall reduced water stress concomitant with increased growth, followed by a gradual increase in water stress (i.e. ^{13}C -enrichment) in the later stages of the experiment, which paired with a growth decline (Figure 2c,d). While the $\delta^{13}C$ values were not significantly different between the two vitality levels, TRW values of IH and IL trees were significantly different, indicating incongruences between stomatal and photosynthetic responses (Schönbeck et al., 2022), or different carbon allocation strategies between vitality levels (Figure 2c; Figure S5). This suggests that the irrigated trees were unable to meet the increased water demand from the increased biomass, leading to a scaling back of tree growth over time. Similar results are shown in Giuggiola et al. (2013), where a positive thinning-induced growth release in Scots pine disappeared after approximately two decades.

Based on the findings of our multi-proxy approach, we conclude that the irrigation-induced growth overyielding could not be sustained because new boundary conditions of water limitations were reached (Schönbeck et al., 2022). In this third phase, the soil water content measurements of irrigated and control plots converged because of the greater root biomass and larger rooting system

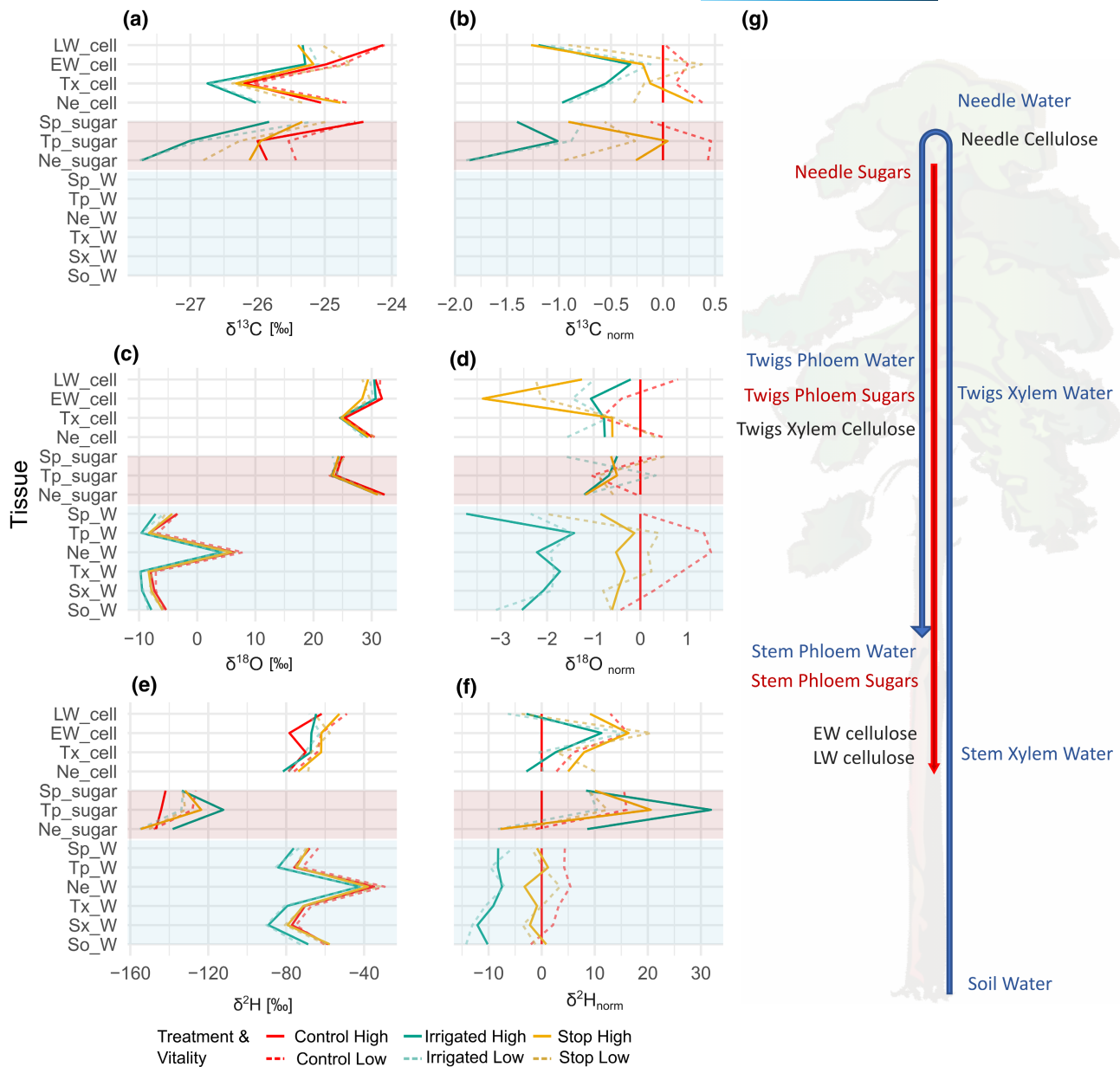


FIGURE 6 Annual averages of (a) $\delta^{13}\text{C}$, (c) $\delta^{18}\text{O}$ and (e) $\delta^2\text{H}$ for the extracted water (W) and organic compounds (sugar and cell) and for a subset of tissues (g): current-year needles (Ne), twig xylem (Tx), twig phloem (Tp), stem xylem (Sx) and phloem (Sp), and earlywood and latewood cellulose (EW_cell, LW_cell) for the two vitality levels (low and high canopy transparency), and the values normalised to high-vitality control trees (b, d, f). Seasonal averages are shown in [Figure S7](#), and significant differences between tissues are explored in [Figures S8–S12](#).

(Brunner et al., 2019; Wang et al., 2023; 75% increase of root biomass [Figure 1](#), Brunner et al., 2019), larger canopy size (40% increase in LAI [Figure 1](#) %), and more dense understorey in the irrigated plots (Bose et al., 2022) resulted in stronger water demand. This led to soil water availability even lower than that in irrigated plots during spring, i.e. before the annual irrigation cycle started (D'Odorico et al., 2021). These results are in line with those from Barbeta et al. (2013), where the effect of irrigation declined after a decade of increased water availability. Further, they support the hypothesis that the response to a release from water limitation tends to involve an initial overshooting of growth before new limiting factors, such

as nutrient availability or new water limitations, constrain growth to rebalance water supply and demand.

4.2 | Stop treatment: Irrigation-induced structural overbuilding and physiological imbalance

When trees physiologically and structurally have acclimated to a new equilibrium as a result of improved water availability, the sudden stop of this additional water impacts them differently than control trees. Over the 4 years without irrigation, the trees in the

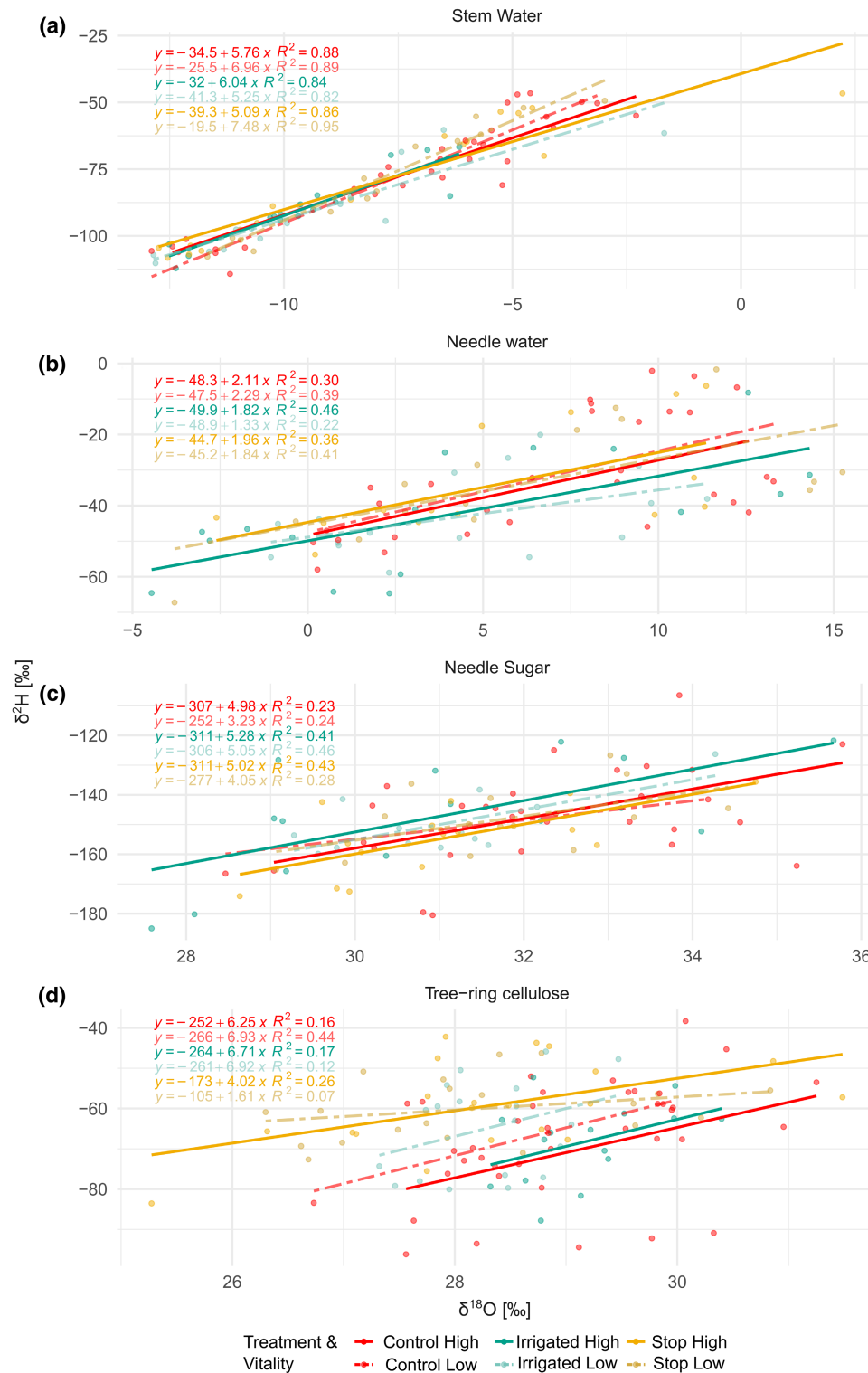


FIGURE 7 O-H relationship, fitted linear models ($y=b+ax$, where b =intercept and a =slope) and R^2 for (a) xylem water, (b) needle water and (c) and needle sugars in the vegetative phase of 2019 and for (d) tree-ring cellulose during assimilation phase 3 for the three treatments and the two vitality levels. The O-H relationship in the previous two phases is shown in [Figure S13](#).

stop treatment declined considerably in stem growth. They reached pre-irrigation stem radial growth levels after about 4 years that were comparable to those of CL trees, indicating the penalty of sustaining the irrigation-induced structural overbuilding (e.g. increase

above- and below-ground biomass, [Figure 1](#)) once water became scarce again. This was especially the case for the high-vitality trees, which showed the most canopy expansion and radial growth (TRW) in response to irrigation, and the steepest decline after irrigation

stopped (Figure 3). This finding is confirmed by the shift in wood tissue traits, with stop trees not only having the shortest cell maturation period but also producing the smallest number of cells and having the lowest hydraulic conductivity (Figure 4). Similar results were found in another 'irrigation-stop' experiment in a Scots pine forest, where radial growth declined dramatically after the sudden reduction in water availability; in that case, however, the growth rates did not return to the levels of the control trees after irrigation stopped (Rigling et al., 2003).

The isotopic measurements in this growth-declining phase showed a different picture. The OH relationship for the Stop trees was the weakest, indicating functioning under severely limiting conditions and the ongoing process of acclimation. We infer this from recent advanced understanding of the decoupling between the two isotope ratios after disturbance, as found after defoliation by insects (Vitali et al., 2023). However, we see a better OH relationship in SH trees indicating that they grow under more favourable conditions, likely during the early part of the vegetative season, as suggested by the low $\delta^{13}\text{C}$. At the onset of the stop treatment in 2014, the SH trees' $\delta^{13}\text{C}$ values were similar to those of the irrigated trees (Figure 3c,d). The SH trees still had $\delta^{13}\text{C}$ values similar to those of IH trees in 2019, indicating that the SH trees might have maintained canopy functioning similar to that of the irrigated trees (i.e. stomatal conductance and photosynthetic rate). This information, paired with the high sap flow in spring and early summer for the SH trees (Zweifel et al., 2020), suggests that these trees had not yet adjusted their canopy functioning to match the reduced water availability. The lack of higher $\delta^{13}\text{C}$ values in SH trees, which would have indicated a stress response, might be due to the early cessation of new cell formation in the later part of the vegetative season (Figure 4). Hunziker et al. (2022) showed that especially late summer water restrictions induce a stress response in Scots pine in the Swiss Rhone valley, at a time when the SH trees had already ceased cell production. On the contrary, the SL trees appear to have a different acclimation strategy, as their TRW trees remained more constant, albeit very low, between phase 2 and 3, their $\delta^{13}\text{C}$ values gradually converged to the values of the control trees even before irrigation stopped (Figure 3c,d), indicating increasing water use efficiency. Our multi-proxy investigation clearly shows the differences in timing and responses to the stop treatment regarding growth and tree physiology, while also highlighting the strong physiological differences between tree vitality levels (Hp2).

We also found that the length of legacy effect after irrigation stopped differed for different leaf and wood traits. In particular, we observed: (i) higher photosynthesis and stomatal conductance in the stop trees than in the control trees, and maximum carboxylation and electron transport rates in 2019 that were similar to the pre-irrigation (before 2003) levels (Schönbeck et al., 2022); (ii) lower crown transparency in stop trees compared with the control trees still in 2020; and (iii) a relatively low stress level as indicated by the photochemical reflectance index (D'Odorico et al., 2021). Meanwhile, shorter new needles, reduced annual sap flow (Zweifel et al., 2020) and lower xylem production (Figure 2a) indicated a negative effect of the stop

treatment. This aligns with the assumption that Scots pine trees are slow responders to changes in environmental conditions (Zweifel & Sterck, 2018), due to their species-specific characteristics, including needle generation times of up to 4–5 years. In the case of the irrigated trees, it took 10 years to return to pre-irrigation growth dynamics, and thus it follows that the stop trees should still be acclimating in the 5 years after irrigation stopped (Hp1b). Furthermore, if these trends continue, these strongly reduced growth levels could become a precursor to mortality, as dying trees have been shown to switch to more conservative hydraulic strategies and higher water-use efficiency (Figure 2), leading to an insufficient supply of carbohydrates, less stem growth and reduced needle mass (Timofeeva et al., 2017).

4.3 | Tree functioning affects water isotope variation

Here we consider physical and biochemical mechanisms that could have affected the isotope signals along the biosynthetic pathway. In general, $\delta^{18}\text{O}$ and $\delta^2\text{H}$ tend to vary in parallel and are therefore positively correlated, not only in water but also in organic matter (Sanchez-Bragado et al., 2019). However, we observed a gradual degradation of the O–H relationship along the plant biosynthetic pathway from source water to needle sugars and tree-ring cellulose, as well as significant differences among the treatments.

4.3.1 | Source and needle water

All treatments showed a consistent hydrological O–H relationship in the soil and xylem water (similar slopes and R^2 values; Figure 7a), with differences in the soil water isotopic signature between the irrigated and control treatments (Figure 5a) occurring due to the isotopically depleted irrigation water. Differences between the absolute values of xylem water between vitality levels might indicate differences in rooting and water uptake depths (Figures 6 and 7a; Figure S7; Freyberg et al., 2020). In the needles, we observed the expected isotopic enrichment induced by canopy transpiration and atmospheric exchange (Figure 6; e.g., Cernusak et al., 2022; Craig & Gordon, 1965; Farquhar & Lloyd, 1993). Here, the depleted levels in the irrigated trees became non-significantly different from those in the control trees, suggesting that a stronger positive fractionation impacted the isotopic signatures in the needle water of irrigated trees. This could be attributed to temperature-dependent fractionation of larger needles (Timofeeva et al., 2020).

4.3.2 | Needle sugars

Treatment-induced differences in needle size and water availability also affect needle sugar formation, as assimilation is regulated by stomata and temperature (Helliker & Richter, 2008; Leppä

et al., 2022). The temperature response curves in our study show how $\delta^{18}\text{O}$ and $\delta^2\text{H}$ had opposite responses to increasing temperature (Figure S14), inducing a stronger O–H decoupling (lower R^2 values) in control trees, which were more negatively affected by the high temperatures due to their small needles and the low water availability. Furthermore, during organic synthesis, many water-availability-dependent reactions can induce additional variation in both $\delta^2\text{H}$ and $\delta^{18}\text{O}$ (Holloway-Phillips et al., 2023; Luo & Sternberg, 1992; Martínez-Sancho et al., 2023).

4.3.3 | Tree-ring cellulose

The O–H relationship in the tree-ring cellulose of the irrigated and control trees became significantly different from that of the needle sugars and once again more similar to the hydrological signal carried by the xylem water (compare the slope terms in Figure 7a,d). There is evidence that time lags between transport and assimilation of sugars (Gessler et al., 2009), along with increased sugar residence time in sink cells, enhance metabolite cycling and isotopic exchange of O (Barnard et al., 2007; Song et al., 2014) and H (Augusti et al., 2006) with xylem water. These processes could be responsible for the re-imprinting of the hydrological signature during tree-ring formation (Augusti et al., 2008; Gessler et al., 2013), especially under periods of high evaporative demand (Martínez-Sancho et al., 2023). This phenomenon arises from the repetitive cycling of sugars, which increases the opportunity for O and H isotope exchanges (Barbour & Farquhar, 2000; Cormier et al., 2018; Song et al., 2014) and finally results in a re-imprinting of the hydrological signature. This suggests a similar latency time in the irrigated and control trees (for the pairs CH–IH and CL–IL), which share similar O–H relationships. Meanwhile, the irrigation-induced increase in total biomass of the stop trees created an increased respiratory demand for sugars, which could not be sustained due to the decline in assimilation rate after irrigation stopped (Schönbeck et al., 2022). In this case, the sugar latency time in the stem might have been shorter and the glucose C–H groups might have exchanged only weakly with the xylem water, thus retaining the $\delta^2\text{H}$ values established in the leaf sugars, reflecting different metabolic reactions (Augusti et al., 2008; Holloway-Phillips et al., 2023).

4.4 | Identification of acclimation balance and turning points

The process of determining acclimation either at the stand level or at the tree level depends on both temporal and spatial resolution. However, we can consider a forest stable when there is similar functioning among the trees, thus being in equilibrium with available resources. We hypothesised that a stronger relationship between $\delta^{18}\text{O}$ and $\delta^2\text{H}$ in tree-ring cellulose would suggest that tree functions are operating near an equilibrium state, retaining a stronger

hydrological rather than a biochemical isotope signature. By contrast, when trees are functioning in a perturbed state [e.g. changes in nutrient, water and light availability (Lehmann et al., 2021), or in case of defoliation events induced by pests and diseases (Vitali et al., 2023)], metabolism will become more variable, attempting to compensate for the new growing conditions, and thus the physiological signals will overwrite the O–H relationship (lower R^2 values indicates lower population-level agreement). Based on typical responses of plants to perturbations, we assume that the response norm follows a sigmoid curve as stress increases, translating to a bell-shaped distribution of population-level variability (Figure 8a,b; e.g. Anderegg, 2015; Pammenter & Vander Willigen, 1998). Thus, in an equilibrium state plants are in physiological balance, functioning 'normally' until the pressure from the stressor reaches a turning point where the metabolic functioning of the tree changes, resulting in greater variability within the population. Eventually, a new equilibrium is achieved at a different functional state, which could even indicate mortality in the worst-case scenario. In our case, the irrigated trees represent the top left quadrant in Figure 8a, with high growth rates (TRW) and low $\delta^{13}\text{C}$ values (i.e. low-stress conditions) and a coupling of O and H isotopes, indicating an equilibrium state. The stop trees would fall in the transition zone, as we observed the strongest O–H isotope decoupling in this treatment (indicated by the lowest R^2 values, i.e. the highest variability between trees and years), paired with low TRW, pointing to an increase in stress conditions. However, the SH trees had low $\delta^{13}\text{C}$ values, suggesting that they were closer to the irrigated trees along the stress gradient, while SL trees would be closer to the control trees. The control trees would fall at the bottom of the sigmoid curve (Figure 8a), with low TRW and high $\delta^{13}\text{C}$ showing stressful growth conditions but at an acclimated state, as shown by the coupling of the O and H isotopes. These results confirm Hp3, that the O–H relationship of tree-ring stable isotopes can be used as a proxy for the extent of acclimation status of the population.

5 | CONCLUSIONS

Climate change is expected to bring fast and unprecedented shifts in water availability across Europe, with potential impacts on the performance and survival of forests, thereby challenging the resilience of ecosystems. Acclimation processes offer a rapid response to such climate changes; however, their dynamics and interactions over time, which are also species-specific, remain inadequately understood. Currently, isotopes are used to retrospectively assess the triggers of tree mortality (Gessler et al., 2018). With this study, we could show that by using a multi-proxy approach we combine data from different tree compartments, and time resolutions creating a comprehensive, growth-weighted evaluation of tree physiology, stages of acclimation or shifts between steady states. Thus, this information could be used as an early warning sign of an unbalanced ecosystem shifting towards a lower functioning state, and when the acclimation processes are insufficient, mortality. The limited

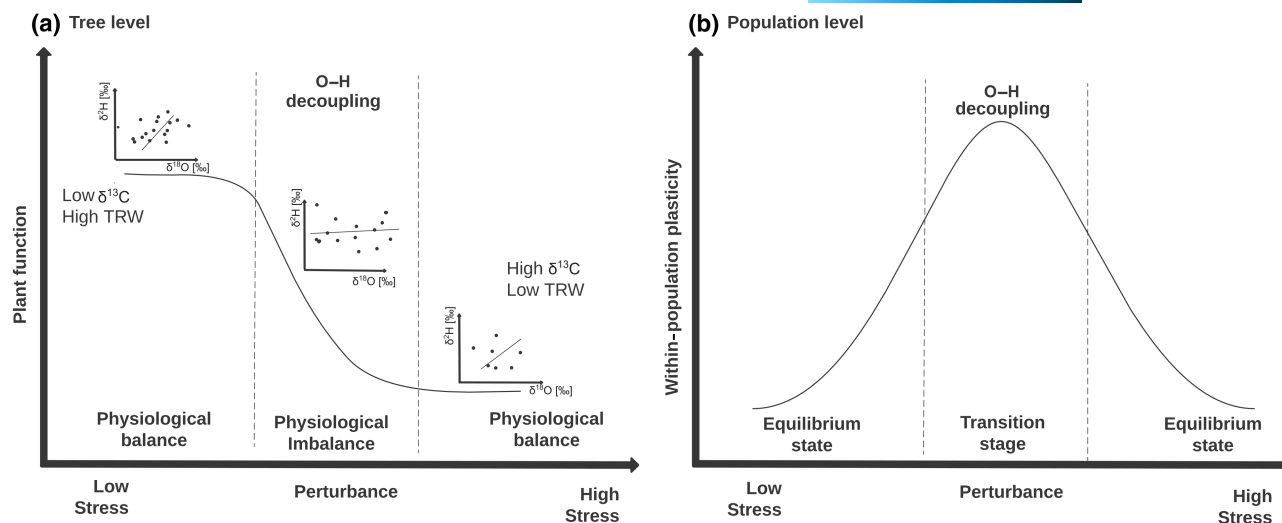


FIGURE 8 Schematic representation of tree functioning along a gradient of increasing perturbation that induces shifts from trees growing in physiological balance (O–H isotope coupling) to (a) physiological imbalance and (b) higher population variability (O–H isotope decoupling).

number of long-term irrigation experiments hinders the generalisation of observed patterns, clearly underscoring the importance of the ongoing water manipulation experiment in the dry forest of Pfywald, multi-annual monitoring, and the necessity for whole-stand investigations to grasp the intricate acclimation dynamics of the forest system. From this investigation, we conclude that trees acclimated to constant irrigation levels over the course of more than a decade and that the sudden removal of irrigation strongly impacted the tree functioning, triggering physiological imbalance and a new cascade of ongoing acclimation processes.

AUTHOR CONTRIBUTIONS

Valentina Vitali: Conceptualization; data curation; formal analysis; investigation; methodology; project administration; visualization; writing – original draft; writing – review and editing. **Philipp Schuler:** Investigation; methodology; resources; writing – review and editing. **Meisha Holloway-Phillips:** Conceptualization; formal analysis; visualization; writing – original draft; writing – review and editing. **Petra D'Odorico:** Investigation; writing – review and editing. **Claudia Guidi:** Investigation; writing – original draft; writing – review and editing. **Stefan Klesse:** Formal analysis; writing – original draft; writing – review and editing. **Marco M. Lehmann:** Investigation; writing – original draft; writing – review and editing. **Katrin Meusburger:** Investigation; writing – original draft; writing – review and editing. **Marcus Schaub:** Investigation; writing – review and editing. **Roman Zweifel:** Investigation; writing – original draft; writing – review and editing. **Arthur Gessler:** Conceptualization; supervision; writing – original draft; writing – review and editing. **Matthias Saurer:** Conceptualization; data curation; investigation; methodology; project administration; resources; supervision; writing – original draft; writing – review and editing.

ACKNOWLEDGEMENTS

We thank Manuela Oetli and Oliver Rehmann for help with sample preparation and processing, and Jonas Gisler for his work in maintaining the irrigation system at Pfywald. We thank Melissa Dawes

for her help editing the manuscript. Open access funding provided by ETH-Bereich Forschungsanstalten.

FUNDING INFORMATION

This study was supported by the Swiss National Science Foundation (SNSF) with the following projects. VV and MS: SNF project 200020_182092; MHP: TreeWater (No. 205492); CG: European Union's Horizon 2020 research and innovation programme and Marie Skłodowska-Curie grant agreement No 846134; MML: SNF Ambizione project TreeCarbo (No. 179978); AG: SNF project 310030_189109.

CONFLICT OF INTEREST STATEMENT

The authors declare that the research was conducted in the absence of any commercial or financial relationships that could be construed as a potential conflict of interest.

DATA AVAILABILITY STATEMENT

The data that support the findings of this study are openly available in the ENVIDAT database at <https://www.doi.org/10.16904/envidat.480>.

ORCID

Valentina Vitali <https://orcid.org/0000-0002-3045-6178>
 Philipp Schuler <https://orcid.org/0000-0002-5711-2535>
 Meisha Holloway-Phillips <https://orcid.org/0000-0002-8353-3536>
 Petra D'Odorico <https://orcid.org/0000-0001-9954-8508>
 Claudia Guidi <https://orcid.org/0000-0003-3947-808X>
 Stefan Klesse <https://orcid.org/0000-0003-1569-1724>
 Marco M. Lehmann <https://orcid.org/0000-0003-2962-3351>
 Katrin Meusburger <https://orcid.org/0000-0003-4623-6249>
 Marcus Schaub <https://orcid.org/0000-0002-0158-8892>
 Roman Zweifel <https://orcid.org/0000-0001-9438-0582>
 Arthur Gessler <https://orcid.org/0000-0002-1910-9589>
 Matthias Saurer <https://orcid.org/0000-0002-3954-3534>

REFERENCES

- Anderegg, W. R. (2015). Spatial and temporal variation in plant hydraulic traits and their relevance for climate change impacts on vegetation. *New Phytologist*, 205, 1008–1014.
- Anderegg, W. R., Schwalm, C., Biondi, F., Camarero, J. J., Koch, G., Litvak, M., Ogle, K., Shaw, J. D., Shevliakova, E., Williams, A. P., Wolf, A., Ziaco, E., & Pacala, S. (2015). FOREST ECOLOGY. Pervasive drought legacies in forest ecosystems and their implications for carbon cycle models. *Science (New York, N.Y.)*, 349, 528–532.
- Andreu-Hayles, L., Ummenhofer, C. C., Barriendos, M., Schleser, G. H., Helle, G., Leuenberger, M., Gutiérrez, E., & Cook, E. R. (2017). 400 years of summer hydroclimate from stable isotopes in Iberian trees. *Climate Dynamics*, 49, 143–161.
- Anfodillo, T., & Olson, M. E. (2021). Tree mortality: Testing the link between drought, embolism vulnerability, and xylem conduit diameter remains a priority. *Frontiers in Forests and Global Change*, 4, 704670.
- Atkin, O. (2003). Thermal acclimation and the dynamic response of plant respiration to temperature. *Trends in Plant Science*, 8, 343–351.
- Augusti, A., Betson, T. R., & Schleucher, J. (2006). Hydrogen exchange during cellulose synthesis distinguishes climatic and biochemical isotope fractionations in tree rings. *New Phytologist*, 172, 490–499.
- Augusti, A., Betson, T. R., & Schleucher, J. (2008). Deriving correlated climate and physiological signals from deuterium isotopomers in tree rings. *Chemical Geology*, 252, 1–8.
- Barbeta, A., Ogaya, R., & Peñuelas, J. (2013). Dampening effects of long-term experimental drought on growth and mortality rates of a Holm oak forest. *Global Change Biology*, 19, 3133–3144.
- Barbour, M. M., & Farquhar, G. D. (2000). Relative humidity- and ABA-induced variation in carbon and oxygen isotope ratios of cotton leaves. *Plant, Cell and Environment*, 23, 473–485.
- Barnard, R. L., Salmon, Y., Kodama, N., Sörgel, K., Holst, J., Rennenberg, H., Gessler, A., & Buchmann, N. (2007). Evaporative enrichment and time lags between delta18O of leaf water and organic pools in a pine stand. *Plant, Cell and Environment*, 30, 539–550.
- Bauhus, J., Forrester, D. I., Gardiner, B., Jactel, H., Vallejo, R., & Pretzsch, H. (2017). Ecological stability of mixed-species forests. In H. Pretzsch, D. I. Forrester, & J. Bauhus (Eds.), *Mixed-species forests* (pp. 337–382). Springer.
- Beaman, J. E., White, C. R., & Seebacher, F. (2016). Evolution of plasticity: Mechanistic link between development and reversible acclimation. *Trends in Ecology & Evolution*, 31, 237–249. <https://www.sciencedirect.com/science/article/pii/S0169534716000185>
- Beier, C., Gundersen, P., Hansen, K., & Rasmussen, L. (1995). Experimental manipulation of water and nutrient input to a Norway spruce plantation at Klosterhede, Denmark. *Plant and Soil*, 168–169, 613–622.
- Belluau, M., Vitali, V., Parker, W. C., Paquette, A., & Messier, C. (2021). Overyielding in young tree communities does not support the stress-gradient hypothesis and is favoured by functional diversity and higher water availability. *Journal of Ecology*, 109, 1790–1803.
- Boettger, T., Haupt, M., Knöller, K., Weise, S. M., Waterhouse, J. S., Rinne, K. T., Loader, N. J., Sonninen, E., Jungner, H., Masson-Delmotte, V., Stievenard, M., Guillemin, M. T., Pierre, M., Pazdur, A., Leuenberger, M., Filot, M., Saurer, M., Reynolds, C. E., Helle, G., & Schleser, G. H. (2007). Wood cellulose preparation methods and mass spectrometric analyses of $\delta^{13}\text{C}$ and $\delta^{18}\text{O}$, and nonexchangeable $\delta^2\text{H}$ values in cellulose, sugar, and starch: An interlaboratory comparison. *Analytical Chemistry*, 79, 4603–4612.
- Bose, A. K., Rigling, A., Gessler, A., Hagedorn, F., Brunner, I., Feichtinger, L., Bigler, C., Egli, S., Etzold, S., Gossner, M. M., Guidi, C., Lévesque, M., Meusburger, K., Peter, M., Saurer, M., Scherrer, D., Schleppei, P., Schönbeck, L., Vogel, M. E., ... Schaub, M. (2022). Lessons learned from a long-term irrigation experiment in a dry Scots pine forest: impacts on traits and functioning. *Ecological Monographs*, 92, e1507.
- Bréda, N., Huc, R., Granier, A., & Dreyer, E. (2006). Temperate forest trees and stands under severe drought: A review of ecophysiological responses, adaptation processes and long-term consequences. *Annals of Forest Science*, 63, 625–644.
- Brunner, I., Herzog, C., Galiano, L., & Gessler, A. (2019). Plasticity of fine-root traits under long-term irrigation of a water-limited Scots pine forest. *Frontiers in Plant Science*, 10, 701.
- Brunner, I., Pannatier, E. G., Frey, B., Rigling, A., Landolt, W., Zimmermann, S., & Dobbertin, M. (2009). Morphological and physiological responses of Scots pine fine roots to water supply in a dry climatic region in Switzerland. *Tree Physiology*, 29, 541–550.
- Bunn, A. G. (2010). Statistical and visual crossdating in R using the dplR library. *Dendrochronologia*, 28, 251–258.
- Cabon, A., Peters, R. L., Fonti, P., Martínez-Vilalta, J., & De Cáceres, M. (2020). Temperature and water potential co-limit stem cambial activity along a steep elevational gradient. *New Phytologist*, 226, 1325–1340.
- Cernusak, L. A., Barbeta, A., Bush, R. T., Eichstaedt (Bögelein), R., Ferrio, J. P., Flanagan, L. B., Gessler, A., Martín-Gómez, P., Hirl, R. T., Kahmen, A., Keitel, C., Lai, C. T., Munksgaard, N. C., Nelson, D. B., Ogée, J., Roden, J. S., Schnyder, H., Voelker, S. L., Wang, L., ... Cuntz, M. (2022). Do ^2H and ^{18}O in leaf water reflect environmental drivers differently? *New Phytologist*, 235, 41–51.
- Chen, Z., Li, S., Wan, X., & Liu, S. (2022). Strategies of tree species to adapt to drought from leaf stomatal regulation and stem embolism resistance to root properties. *Frontiers in Plant Science*, 13, 926535.
- Cook, E. R., & Kairiukstis, L. A. (1990). *Methods of dendrochronology. Applications in the environmental sciences* (p. 394). Springer Netherlands.
- Cormier, M.-A., Werner, R. A., Sauer, P. E., Gröcke, D. R., Leuenberger, M. C., Wieloch, T., Schleucher, J., & Kahmen, A. (2018). ^2H -fractionations during the biosynthesis of carbohydrates and lipids imprint a metabolic signal on the $\delta^2\text{H}$ values of plant organic compounds. *New Phytologist*, 218, 479–491.
- Cotrufo, M. F., Alberti, G., Inglima, I., Marjanović, H., LeCain, D., Zaldei, A., Peressotti, A., & Miglietta, F. (2011). Decreased summer drought affects plant productivity and soil carbon dynamics in a Mediterranean woodland. *Biogeosciences*, 8, 2729–2739.
- Craig, H., & Gordon, I. I. (1965). Deuterium and oxygen 18 variations in the ocean and the marine atmosphere. In E. Tongiogi & V. Lishi e F., (Eds.), *Stable isotopes in oceanographic studies and paleotemperatures*. (pp. 9–130). Consiglio nazionale delle ricerche, Laboratorio di geologia nucleare.
- Cuny, H. E., Fonti, P., Rathgeber, C. B., von Arx, G., Peters, R. L., & Frank, D. C. (2019). Couplings in cell differentiation kinetics mitigate air temperature influence on conifer wood anatomy. *Plant, Cell and Environment*, 42, 1222–1232.
- da Costa, A. C. L., Rowland, L., Oliveira, R. S., Oliveira, A. A. R., Binks, O. J., Salmon, Y., Vasconcelos, S. S., Junior, J. A. S., Ferreira, L. V., Poyatos, R., Mencuccini, M., & Meir, P. (2018). Stand dynamics modulate water cycling and mortality risk in droughted tropical forest. *Global Change Biology*, 24, 249–258.
- Dansgaard, W. (1964). Stable isotopes in precipitation. *Tellus*, 16, 436–468.
- Diao, H., Schuler, P., Goldsmith, G. R., Siegwolf, R. T., Saurer, M., & Lehmann, M. M. (2022). Technical note: On uncertainties in plant water isotopic composition following extraction by cryogenic vacuum distillation. *Hydrology and Earth System Sciences*, 26, 5835–5847.
- Dobbertin, M., Eilmann, B., Bleuler, P., Giuggiola, A., Graf Pannatier, E., Landolt, W., Schleppei, P., & Rigling, A. (2010). Effect of irrigation on needle morphology, shoot and stem growth in a drought-exposed Pinus sylvestris forest. *Tree Physiology*, 30, 346–360.
- Dobbertin, M., Hug, C., & Mizoue, N. (2004). Using slides to test for changes in crown defoliation assessment methods. Part I: Visual assessment of slides. *Environmental Monitoring and Assessment*, 98, 295–306.

- D'Odorico, P., Schönbeck, L., Vitali, V., Meusburger, K., Schaub, M., Ginzler, C., Zweifel, R., Velasco, V. M. E., Gislér, J., Gessler, A., & Ensminger, I. (2021). Drone-based physiological index reveals long-term acclimation and drought stress responses in trees. *Plant, Cell & Environment*, *44*, 3552–3570.
- Dongmann, G., Nürnberg, H. W., Förstel, H., & Wägener, K. (1974). On the enrichment of $H_2^{18}O$ in the leaves of transpiring plants. *Radiation and Environmental Biophysics*, *11*, 41–52.
- Eilmann, B., Dobbertin, M., & Rigling, A. (2013). Growth response of Scots pine with different crown transparency status to drought release. *Annals of Forest Science*, *70*, 685–693.
- Eilmann, B., Zweifel, R., Buchmann, N., Graf Pannatier, E., & Rigling, A. (2011). Drought alters timing, quantity, and quality of wood formation in Scots pine. *Journal of Experimental Botany*, *62*, 2763–2771.
- Farquhar, G. D., Cernusak, L. A., & Barnes, B. (2007). Heavy water fractionation during transpiration. *Plant Physiology*, *143*, 11–18.
- Farquhar, G. D., & Lloyd, J. (1993). Carbon and oxygen isotope effects in the exchange of carbon dioxide between terrestrial plants and the atmosphere. In J. R. Ehleringer, A. E. Hall & G. D. Farquhar (Eds.), *Stable isotopes and plant carbon-water relations* (pp. 47–70). Elsevier.
- Farquhar, G. D., O'Leary, M. H., & Berry, J. A. (1982). On the relationship between carbon isotope discrimination and the intercellular carbon dioxide concentration in leaves. *Functional Plant Biology*, *9*, 121.
- Faticchi, S., Leuzinger, S., & Körner, C. (2014). Moving beyond photosynthesis: From carbon source to sink-driven vegetation modeling. *New Phytologist*, *201*, 1086–1095.
- Feichtinger, L. M., Eilmann, B., Buchmann, N., & Rigling, A. (2014). Growth adjustments of conifers to drought and to century-long irrigation. *Forest Ecology and Management*, *334*, 96–105.
- Fonti, P., von Arx, G., García-González, I., Eilmann, B., Sass-Klaassen, U., Gärtner, H., & Eckstein, D. (2010). Studying global change through investigation of the plastic responses of xylem anatomy in tree rings. *New Phytologist*, *185*, 42–53.
- Frank, D. C., Poulter, B., Saurer, M., Esper, J., Huntingford, C., Helle, G., Treydte, K., Zimmermann, N. E., Schleser, G. H., Ahlström, A., Ciais, P., Friedlingstein, P., Levis, S., Lomas, M., Sitch, S., Viovy, N., Andreu-Hayles, L., Bednarz, Z., Berninger, F., ... Weigl, M. (2015). Water-use efficiency and transpiration across European forests during the Anthropocene. *Nature Climate Change*, *5*, 579–583.
- Freyberg, J., Allen, S. T., Grossiord, C., & Dawson, T. E. (2020). Plant and root-zone water isotopes are difficult to measure, explain, and predict: Some practical recommendations for determining plant water sources. *Methods in Ecology and Evolution*, *11*, 1352–1367.
- Gavinet, J., Ourcival, J.-M., & Limousin, J.-M. (2019). Rainfall exclusion and thinning can alter the relationships between forest functioning and drought. *New Phytologist*, *223*, 1267–1279.
- Gebhardt, T., Hesse, B. D., Hikino, K., Kolovrat, K., Hafner, B. D., Grams, T. E., & Häberle, K.-H. (2023). Repeated summer drought changes the radial xylem sap flow profile in mature Norway spruce but not in European beech. *Agricultural and Forest Meteorology*, *329*, 109285.
- Gessler, A., Bottero, A., Marshall, J., & Arend, M. (2020). The way back: Recovery of trees from drought and its implication for acclimation. *The New Phytologist*, *228*, 1704–1709.
- Gessler, A., Brandes, E., Buchmann, N., Helle, G., Rennenberg, H., & Barnard, R. L. (2009). Tracing carbon and oxygen isotope signals from newly assimilated sugars in the leaves to the tree-ring archive. *Plant, Cell & Environment*, *32*, 780–795.
- Gessler, A., Brandes, E., Keitel, C., Boda, S., Kayler, Z. E., Granier, A., Barbour, M., Farquhar, G. D., & Treydte, K. (2013). The oxygen isotope enrichment of leaf-exported assimilates – Does it always reflect lamina leaf water enrichment? *New Phytologist*, *200*, 144–157.
- Gessler, A., Caillet, M., Joseph, J., Schönbeck, L., Schaub, M., Lehmann, M., Treydte, K., Rigling, A., Timofeeva, G., & Saurer, M. (2018). Drought induced tree mortality – a tree-ring isotope based conceptual model to assess mechanisms and predispositions. *The New Phytologist*, *219*, 485–490.
- Gessler, A., Rennenberg, H., & Keitel, C. (2004). Stable isotope composition of organic compounds transported in the phloem of European Beech – Evaluation of different methods of phloem sap collection and assessment of gradients in carbon isotope composition during leaf-to-stem transport. *Plant Biology (Stuttgart, Germany)*, *6*, 721–729.
- Giuggiola, A., Bugmann, H., Zingg, A., Dobbertin, M., & Rigling, A. (2013). Reduction of stand density increases drought resistance in xeric Scots pine forests. *Forest Ecology and Management*, *310*, 827–835.
- Gleason, S. M., Westoby, M., Jansen, S., Choat, B., Hacke, U. G., Pratt, R. B., Bhaskar, R., Brodribb, T. J., Bucci, S. J., Cao, K. F., Cochard, H., Delzon, S., Domec, J. C., Fan, Z. X., Feild, T. S., Jacobsen, A. L., Johnson, D. M., Lens, F., Maherali, H., ... Zanne, A. E. (2016). Weak tradeoff between xylem safety and xylem-specific hydraulic efficiency across the world's woody plant species. *New Phytologist*, *209*, 123–136.
- Goke, A., & Martin, P. H. (2022). Poor acclimation to experimental field drought in subalpine forest tree seedlings. *AoB Plants*, *14*, plab077.
- Grams, T. E., Hesse, B. D., Gebhardt, T., Weigl, F., Rötzer, T., Kovacs, B., Hikino, K., Hafner, B. D., Brunn, M., Bauerle, T., Häberle, K.-H., Pretzsch, H., & Pritsch, K. (2021). The Kroof experiment: Realization and efficacy of a recurrent drought experiment plus recovery in a beech/spruce forest. *Ecosphere*, *12*, 3399–3418.
- Grossiord, C. (2020). Having the right neighbors: how tree species diversity modulates drought impacts on forests. *New Phytologist*, *228*(1), 42–49.
- Guerrieri, R., Belmecheri, S., Ollinger, S. V., Asbjornsen, H., Jennings, K., Xiao, J., Stocker, B. D., Martin, M., Hollinger, D. Y., Bracho-Garrillo, R., Clark, K., Dore, S., Kolb, T., Munger, J. W., Novick, K., & Richardson, A. D. (2019). Disentangling the role of photosynthesis and stomatal conductance on rising forest water-use efficiency. *Proceedings of the National Academy of Sciences of the United States of America*, *116*, 16909–16914.
- Hayes, J. M. (2001). 3. Fractionation of carbon and hydrogen isotopes in biosynthetic processes. In J. W. Valley & D. R. Cole (Eds.), *Stable isotope geochemistry* (pp. 225–278). De Gruyter.
- Helliker, B. R., & Richter, S. L. (2008). Subtropical to boreal convergence of tree-leaf temperatures. *Nature*, *454*, 511–514.
- Holloway-Phillips, M., Baan, J., Nelson, D. B., Lehmann, M. M., Tcherkez, G., & Kahmen, A. (2022). Species variation in the hydrogen isotope composition of leaf cellulose is mostly driven by isotopic variation in leaf sucrose. *Plant, Cell and Environment*, *45*, 2636–2651.
- Holloway-Phillips, M., Cernusak, L. A., Nelson, D. B., Lehmann, M. M., Tcherkez, G., & Kahmen, A. (2023). Covariation between oxygen and hydrogen stable isotopes declines along the path from xylem water to wood cellulose across an aridity gradient. *New Phytologist*, *240*, 1758–1773.
- Holmes, R. (1983). Computer-assisted quality control in tree-ring dating and measurement. *Tree-Ring Bulletin*, *43*, 69–78.
- Houston Durrant, T., de Rigo, D., & Caudullo, G. (2016). *Pinus sylvestris* in Europe: Distribution, habitat, usage and threats. In J. San-Miguel-Ayanz, D. de Rigo, G. Caudullo, T. Houston Durrant, & A. Mauri (Eds.), *European atlas of forest tree species* (e016b94).
- Hunziker, S., Begert, M., Scherrer, S. C., Rigling, A., & Gessler, A. (2022). Below average midsummer to early autumn precipitation evolved into the main driver of sudden scots pine vitality decline in the swiss Rhône Valley. *Frontiers in Forests and Global Change*, *5*. <https://doi.org/10.3389/ffgc.2022.874100>
- Ingrisch, J., & Bahn, M. (2018). Towards a comparable quantification of resilience. *Trends in Ecology & Evolution*, *33*, 251–259.
- IPCC. (2022). Climate change 2022. Mitigation of climate change. In P. R. Shukla, J. Skea, R. Slade, A. Al Khourdajie, R. van Diemen, D. McCollum, M. Pathak, S. Some, P. Vyas, R. Fradera, M. Belkacemi, A. Hasija, G. Lisboa, S. Luz, & J. Malley (Eds.), *Contribution of working*

- group III to the sixth assessment report of the Intergovernmental Panel on Climate Change. Cambridge University Press.
- Joseph, J., Gao, D., Backes, B., Bloch, C., Brunner, I., Gleixner, G., Haeni, M., Hartmann, H., Hoch, G., Hug, C., Kahmen, A., Lehmann, M. M., Li, M. H., Luster, J., Peter, M., Poll, C., Rigling, A., Rissanen, K. A., Ruehr, N. K., ... Gessler, A. (2020). Rhizosphere activity in an old-growth forest reacts rapidly to changes in soil moisture and shapes whole-tree carbon allocation. *Proceedings of the National Academy of Sciences of the United States of America*, *117*, 24885–24892.
- Jump, A. S., & Peñuelas, J. (2005). Running to stand still: Adaptation and the response of plants to rapid climate change. *Ecology Letters*, *8*, 1010–1020.
- Jyske, T., & Hölttä, T. (2015). Comparison of phloem and xylem hydraulic architecture in *Picea abies* stems. *New Phytologist*, *205*, 102–115.
- Kagawa, A., & Battipaglia, G. (2022). Post-photosynthetic carbon, oxygen and hydrogen isotope signal transfer to tree rings—How timing of cell formations and turnover of stored carbohydrates affect intra-annual isotope variations. In R. T. W. Siegwolf, J. R. Brooks, J. Roden, & M. Saurer (Eds.), *Stable isotopes in tree rings: Inferring physiological, climatic and environmental responses* (pp. 429–462). Springer International Publishing.
- Kimak, A. (2015). *Tracing physiological processes of long living tree species and their response on climate change using triple isotope analyses*. Philosophisch-naturwissenschaftliche Fakultät der Universität Bern.
- Klesse, S., von Arx, G., Gossner, M. M., Hug, C., Rigling, A., & Quelo, V. (2021). Amplifying feedback loop between growth and wood anatomical characteristics of *Fraxinus excelsior* explains size-related susceptibility to ash dieback. *Tree Physiology*, *41*, 683–696.
- Kolb, K. J., & Sperry, J. (1999). Transport constraints on water use by the Great Basin shrub, *Artemisia tridentata*. *Plant, Cell and Environment*, *22*, 925–935.
- Körner, C. (2015). Paradigm shift in plant growth control. *Current Opinion in Plant Biology*, *25*, 107–114.
- Lambers, H., Chapin, F. S., & Pons, T. L. (1998). *Plant physiological ecology*. Springer-Verlag.
- Lehmann, M. M., Egli, M., Brinkmann, N., Werner, R. A., Saurer, M., & Kahmen, A. (2020). Improving the extraction and purification of leaf and phloem sugars for oxygen isotope analyses. *Rapid Communications in Mass Spectrometry*, *34*, e8854.
- Lehmann, M. M., Vitali, V., Schuler, P., Leuenberger, M., & Saurer, M. (2021). More than climate: Hydrogen isotope ratios in tree rings as novel plant physiological indicator for stress conditions. *Dendrochronologia*, *65*, 125788.
- Leppä, K., Tang, Y., Ogée, J., Launiainen, S., Kahmen, A., Kolari, P., Sahlstedt, E., Saurer, M., Schiestl-Aalto, P., & Rinne-Garmston, K. T. (2022). Explicitly accounting for needle sugar pool size crucial for predicting intra-seasonal dynamics of needle carbohydrates $\delta^{18}\text{O}$ and $\delta^{13}\text{C}$. *New Phytologist*, *236*, 2044–2060.
- Leuenberger, M. (2007). To what extent can ice core data contribute to the understanding of plant ecological developments of the past? In T. E. Dawson & R. T. W. Siegwolf (Eds.), *Stable isotopes as indicators of ecological change* (pp. 211–233). Academic.
- Levesque, M., Andreu-Hayles, L., Smith, W. K., Williams, A. P., Hobi, M. L., Allred, B. W., & Pederson, N. (2019). Tree-ring isotopes capture interannual vegetation productivity dynamics at the biome scale. *Nature Communications*, *10*, 742.
- Lindner, M., Maroschek, M., Netherer, S., Kremer, A., Barbati, A., Garcia-Gonzalo, J., Seidl, R., Delzon, S., Corona, P., Kolström, M., Lexer, M. J., & Marchetti, M. (2010). Climate change impacts, adaptive capacity, and vulnerability of European forest ecosystems. *Forest Ecology and Management*, *259*, 698–709.
- Loader, N. J., McCarroll, D., Gagen, M., Robertson, I., & Jalkanen, R. (2007). Extracting climatic information from stable isotopes in tree rings. In T. E. Dawson & R. T. W. Siegwolf (Eds.), *Stable isotopes as indicators of ecological change* (pp. 25–48). Academic.
- Loader, N. J., Street-Perrott, F. A., Daley, T. J., Hughes, P. D. M., Kimak, A., Levanič, T., Mallon, G., Mauquoy, D., Robertson, I., Roland, T. P., van Bellen, S., Ziehmer, M. M., & Leuenberger, M. (2015). Simultaneous determination of stable carbon, oxygen, and hydrogen isotopes in cellulose. *Analytical Chemistry*, *87*, 376–380.
- Loewe-Muñoz, V., del Río, R., Delard, C., & Balzarini, M. (2021). Short-term stem diameter variations in irrigated and non-irrigated stone pine (*Pinus pinea* L.) trees in a xeric non-native environment. *Annals of Forest Science*, *78*, 99.
- Luo, Y., & Sternberg, L. D. (1992). Hydrogen and oxygen isotopic fractionation during heterotrophic cellulose synthesis. *Journal of Experimental Botany*, *43*, 47–50.
- Mallard, F., Nolte, V., & Schlötterer, C. (2020). The evolution of phenotypic plasticity in response to temperature stress. *Genome Biology and Evolution*, *12*, 2429–2440.
- Marchin, R. M., Broadhead, A. A., Bostic, L. E., Dunn, R. R., & Hoffmann, W. A. (2016). Stomatal acclimation to vapour pressure deficit doubles transpiration of small tree seedlings with warming. *Plant, Cell and Environment*, *39*, 2221–2234.
- Martínez-Sancho, E., Cernusak, L. A., Fonti, P., Gregori, A., Ullrich, B., Pannatier, E. G., Gessler, A., Lehmann, M. M., Saurer, M., & Treydte, K. (2023). Unenriched xylem water contribution during cellulose synthesis influenced by atmospheric demand governs the intra-annual tree-ring $\delta^{18}\text{O}$ signature. *New Phytologist*, *240*, 1743–1757.
- Martin-Stpaul, N. K., Limousin, J.-M., Vogt-Schilb, H., Rodríguez-Calcerrada, J., Rambal, S., Longepierre, D., & Misson, L. (2013). The temporal response to drought in a Mediterranean evergreen tree: Comparing a regional precipitation gradient and a throughfall exclusion experiment. *Global Change Biology*, *19*, 2413–2426.
- McDowell, N., Pockman, W. T., Allen, C. D., Breshears, D. D., Cobb, N., Kolb, T., Plaut, J., Sperry, J., West, A., Williams, D. G., & Yezzer, E. A. (2008). Mechanisms of plant survival and mortality during drought: Why do some plants survive while others succumb to drought? *New Phytologist*, *178*, 719–739.
- Moreno, M., Simioni, G., Cailleret, M., Ruffault, J., Badel, E., Carrière, S., Davi, H., Gavinet, J., Huc, R., Limousin, J. M., Marloie, O., Martin, L., Rodríguez-Calcerrada, J., Vennetier, M., & Martin-StPaul, N. (2021). Consistently lower sap velocity and growth over nine years of rainfall exclusion in a Mediterranean mixed pine-oak forest. *Agricultural and Forest Meteorology*, *308–309*, 108472.
- Nabeshima, E., Nakatsuka, T., Kagawa, A., Hiura, T., & Funada, R. (2018). Seasonal changes of δD and $\delta^{18}\text{O}$ in tree-ring cellulose of *Quercus crispula* suggest a change in post-photosynthetic processes during earlywood growth. *Tree Physiology*, *38*, 1829–1840.
- Nadal-Sala, D., Grote, R., Birami, B., Knüver, T., Rehschuh, R., Schwarz, S., & Ruehr, N. K. (2021). Leaf shedding and non-stomatal limitations of photosynthesis mitigate hydraulic conductance losses in scots pine saplings during severe drought stress. *Frontiers in Plant Science*, *12*, 715127.
- Nicotra, A. B., Atkin, O. K., Bonser, S. P., Davidson, A. M., Finnegan, E. J., Mathesius, U., Poot, P., Purugganan, M. D., Richards, C. L., Valladares, F., & van Kleunen, M. (2010). Plant phenotypic plasticity in a changing climate. *Trends in Plant Science*, *15*, 684–692.
- Pammenter, N. W., & Vander Willigen, C. (1998). A mathematical and statistical analysis of the curves illustrating vulnerability of xylem to cavitation. *Tree Physiology*, *18*, 589–593.
- Parry, M. A., Andralojc, P. J., Khan, S., Lea, P. J., & Keys, A. J. (2002). Rubisco activity: Effects of drought stress. *Annals of Botany*, *89*, 833–839.
- Peters, R. L., Balanzategui, D., Hurley, A. G., von Arx, G., Prendin, A. L., Cuny, H. E., Björklund, J., Frank, D. C., & Fonti, P. (2018). RAPTOR: Row and position tracheid organizer in *R. Dendrochronologia*, *47*, 10–16.
- Peters, R. L., Steppe, K., Cuny, H. E., de Pauw, D. J. W., Frank, D. C., Schaub, M., Rathgeber, C. B. K., Cabon, A., & Fonti, P. (2021). Turgor

- a limiting factor for radial growth in mature conifers along an elevational gradient. *New Phytologist*, 229, 213–229.
- Prendin, A. L., Mayr, S., Beikircher, B., von Arx, G., & Petit, G. (2018). Xylem anatomical adjustments prioritize hydraulic efficiency over safety as Norway spruce trees grow taller. *Tree Physiology*, 38, 1088–1097.
- Prendin, A. L., Petit, G., Carrer, M., Fonti, P., Björklund, J., & von Arx, G. (2017). New research perspectives from a novel approach to quantify tracheid wall thickness. *Tree Physiology*, 37, 976–983.
- Pretzsch, H., del Río, M., Biber, P., Arcangeli, C., Bielak, K., Brang, P., Dudzinska, M., Forrester, D. I., Klädtke, J., Kohnle, U., Ledermann, T., Matthews, R., Nagel, J., Nagel, R., Nilsson, U., Ningre, F., Nord-Larsen, T., Wernsdörfer, H., & Sycheva, E. (2019). Maintenance of long-term experiments for unique insights into forest growth dynamics and trends: Review and perspectives. *European Journal of Forest Research*, 138, 165–185.
- Pugnaire, F. I., Morillo, J. A., Peñuelas, J., Reich, P. B., Bardgett, R. D., Gaxiola, A., Wardle, D. A., & van der Putten, W. H. (2019). Climate change effects on plant-soil feedbacks and consequences for biodiversity and functioning of terrestrial ecosystems. *Science Advances*, 5, eaaz1834.
- R Core Team. (2022). *R: A language and environment for statistical computing*. R Foundation for Statistical Computing. <https://www.R-project.org/>
- Rigling, A., Brühlhart, H., Bräker, O. U., Forster, T., & Schweingruber, F. H. (2003). Effects of irrigation on diameter growth and vertical resin duct production in *Pinus sylvestris* L. on dry sites in the central Alps, Switzerland. *Forest Ecology and Management*, 175, 285–296.
- Rinne, K. T., Saurer, M., Streit, K., & Siegwolf, R. T. (2012). Evaluation of a liquid chromatography method for compound-specific $\delta^{13}\text{C}$ analysis of plant carbohydrates in alkaline media. *Rapid Communications in Mass Spectrometry*, 26, 2173–2185.
- Rodríguez-Calcerrada, J., Jaeger, C., Limousin, J. M., Ourcival, J. M., Joffre, R., & Rambal, S. (2011). Leaf CO_2 efflux is attenuated by acclimation of respiration to heat and drought in a Mediterranean tree. *Functional Ecology*, 25, 983–995.
- Rossi, S., Anfodillo, T., & Menardi, R. (2006). Trephor: A new tool for sampling microcores from tree stems. *IAWA Journal*, 27, 89–97.
- Rowland, L., Ramírez-Valiente, J.-A., Hartley, I. P., & Mencuccini, M. (2023). How woody plants adjust above- and below-ground traits in response to sustained drought. *New Phytologist*, 239, 1173–1189.
- Sanchez-Bragado, R., Serret, M. D., Marimon, R. M., Bort, J., & Araus, J. L. (2019). The hydrogen isotope composition $\delta^2\text{H}$ reflects plant performance. *Plant Physiology*, 180, 793–812.
- Sangüesa-Barreda, G., Gazol, A., & Camarero, J. J. (2023). Drops in needle production are early-warning signals of drought-triggered dieback in Scots pine. *Trees*, 37, 1137–1151.
- Saurer, M., Aellen, K., & Siegwolf, R. (1997). Correlating $\delta^{13}\text{C}$ and $\delta^{18}\text{O}$ in cellulose of trees. *Plant, Cell and Environment*, 20, 1543–1550.
- Saurer, M., Spahni, R., Frank, D. C., Joos, F., Leuenberger, M., Loader, N. J., McCarroll, D., Gagen, M., Poulter, B., Siegwolf, R. T. W., Andreu-Hayles, L., Boettger, T., Dorado Liñán, I., Fairchild, I. J., Friedrich, M., Gutierrez, E., Haupt, M., Hiltavuori, E., Heinrich, I., ... Young, G. H. F. (2014). Spatial variability and temporal trends in water-use efficiency of European forests. *Global Change Biology*, 20, 3700–3712.
- Scheidegger, Y., Saurer, M., Bahn, M., & Siegwolf, R. (2000). Linking stable oxygen and carbon isotopes with stomatal conductance and photosynthetic capacity: A conceptual model. *Oecologia*, 125, 350–357.
- Schönbeck, L., Gessler, A., Hoch, G., McDowell, N. G., Rigling, A., Schaub, M., & Li, M.-H. (2018). Homeostatic levels of nonstructural carbohydrates after 13 yr of drought and irrigation in *Pinus sylvestris*. *The New Phytologist*, 219, 1314–1324.
- Schönbeck, L., Grossiord, C., Gessler, A., Gisler, J., Meusburger, K., D'Odorico, P., Rigling, A., Salmon, Y., Stocker, B. D., Zweifel, R., & Schaub, M. (2022). Photosynthetic acclimation and sensitivity to short- and long-term environmental changes in a drought prone forest. *Journal of Experimental Botany*, 73, 2576–2588.
- Schuler, P., Cormier, M.-A., Werner, R. A., Buchmann, N., Gessler, A., Vitali, V., Saurer, M., & Lehmann, M. M. (2022). A high-temperature water vapor equilibration method to determine non-exchangeable hydrogen isotope ratios of sugar, starch and cellulose. *Plant, Cell and Environment*, 45, 12–22.
- Song, X., Farquhar, G. D., Gessler, A., & Barbour, M. M. (2014). Turnover time of the non-structural carbohydrate pool influences $\delta^{18}\text{O}$ of leaf cellulose. *Plant, Cell and Environment*, 37, 2500–2507.
- Soudant, A., Loader, N. J., Bäck, J., Levula, J., & Kljun, N. (2016). Intra-annual variability of wood formation and $\delta^{13}\text{C}$ in tree-rings at Hyttälä, Finland. *Agricultural and Forest Meteorology*, 224, 17–29. <https://www.sciencedirect.com/science/article/pii/S0168192316302465>
- Terwilliger, V. J., & Deniro, M. J. (1995). Hydrogen isotope fractionation in wood-producing avocado seedlings: Biological constraints to paleoclimatic interpretations of δD values in tree ring cellulose nitrate. *Geochimica et Cosmochimica Acta*, 59, 5199–5207.
- Timofeeva, G., Treydte, K., Bugmann, H., Rigling, A., Schaub, M., Siegwolf, R., & Saurer, M. (2017). Long-term effects of drought on tree-ring growth and carbon isotope variability in Scots pine in a dry environment. *Tree Physiology*, 37, 1028–1041.
- Timofeeva, G., Treydte, K., Bugmann, H., Salmon, Y., Rigling, A., Schaub, M., Vollenweider, P., Siegwolf, R., & Saurer, M. (2020). How does varying water supply affect oxygen isotope variations in needles and tree rings of Scots pine? *Tree Physiology*, 40, 1366–1380.
- Van Sundert, K., Leuzinger, S., Bader, M. K., Chang, S. X., De Kauwe, M. G., Dukes, J. S., Langley, J. A., Ma, Z., Mariën, B., Reynaert, S., Ru, J., Song, J., Stocker, B., Terrer, C., Thoresen, J., Vanuytrecht, E., Wan, S., Yue, K., & Vicca, S. (2023). When things get MESI: The Manipulation Experiments Synthesis Initiative-A coordinated effort to synthesize terrestrial global change experiments. *Global Change Biology*, 29, 1922–1938.
- Vitali, V., Klesse, S., Weigt, R., Treydte, K., Frank, D., Saurer, M., & Siegwolf, R. T. (2021). High-frequency stable isotope signals in uneven-aged forests as proxy for physiological responses to climate in Central Europe. *Tree Physiology*, 41, 2046–2062.
- Vitali, V., Martínez-Sancho, E., Treydte, K., Andreu-Hayles, L., Dorado-Liñán, I., Gutierrez, E., Helle, G., Leuenberger, M., Loader, N. J., Rinne-Garmston, K. T., Schleser, G. H., Allen, S., Waterhouse, J. S., Saurer, M., & Lehmann, M. M. (2022). The unknown third – Hydrogen isotopes in tree-ring cellulose across Europe. *Science of the Total Environment*, 813, 152281.
- Vitali, V., Peters, R. L., Lehmann, M. M., Leuenberger, M., Treydte, K., Büntgen, U., Schuler, P., & Saurer, M. (2023). Tree-ring isotopes from the swiss Alps reveal non-climatic fingerprints of cyclic insect population outbreaks over the past 700 years. *Tree Physiology*, 43, 706–721.
- von Arx, G., & Carrer, M. (2014). ROXAS – A new tool to build centuries-long tracheid-lumen chronologies in conifers. *Dendrochronologia*, 32, 290–293.
- Wang, S., Gao, X., Yang, M., Huo, G., Song, X., Siddique, K. H., Wu, P., & Zhao, X. (2023). The natural abundance of stable water isotopes method may overestimate deep-layer soil water use by trees. *Hydrology and Earth System Sciences*, 27, 123–137.
- Weigt, R. B., Bräunlich, S., Zimmermann, L., Saurer, M., Grams, T. E., Dietrich, H.-P., Siegwolf, R. T., & Nikolova, P. S. (2015). Comparison of $\delta^{18}\text{O}$ and $\delta^{13}\text{C}$ values between tree-ring whole wood and cellulose in five species growing under two different site conditions. *Rapid Communications in Mass Spectrometry*, 29, 2233–2244.
- Werner, C., Meredith, L. K., Ladd, S. N., Ingrisch, J., Kübert, A., van Haren, J., Bahn, M., Bailey, K., Bamberger, I., Beyer, M., Blomdahl, D., Byron, J., Daber, E., Deleeuw, J., Dippold, M. A., Fudyma, J., Gil-Loaiza, J., Honeker, L. K., Hu, J., ... Williams, J. (2021). Ecosystem fluxes during drought and recovery in an experimental forest. *Science (New York, N.Y.)*, 374, 1514–1518.

- West, A. G., Patrickson, S. J., & Ehleringer, J. R. (2006). Water extraction times for plant and soil materials used in stable isotope analysis. *Rapid Communications in Mass Spectrometry*, *20*, 1317–1321.
- Wieloch, T., Grabner, M., Augusti, A., Serk, H., Ehlers, I., Yu, J., & Schleucher, J. (2022). Metabolism is a major driver of hydrogen isotope fractionation recorded in tree-ring glucose of *Pinus nigra*. *The New Phytologist*, *234*, 449–461.
- Wilson, R. S., & Franklin, C. E. (2002). Testing the beneficial acclimation hypothesis. *Trends in Ecology & Evolution*, *17*, 66–70. <https://www.sciencedirect.com/science/article/pii/S0169534701023849>
- Yakir, D., & DeNiro, M. J. (1990). Oxygen and hydrogen isotope fractionation during cellulose metabolism in *Lemna gibba* L. *Plant Physiology*, *93*, 325–332.
- Zimmermann, J., Link, R. M., Hauck, M., Leuschner, C., & Schuldt, B. (2021). 60-year record of stem xylem anatomy and related hydraulic modification under increased summer drought in ring- and diffuse-porous temperate broad-leaved tree species. *Trees*, *35*, 919–937.
- Zweifel, R., Etzold, S., Sterck, F., Gessler, A., Anfodillo, T., Mencuccini, M., von Arx, G., Lazzarin, M., Haeni, M., Feichtinger, L., Meusburger, K., Knuesel, S., Walthert, L., Salmon, Y., Bose, A. K., Schoenbeck, L., Hug, C., de Girardi, N., Giuggiola, A., ... Rigling, A. (2020). Determinants of legacy effects in pine trees – Implications from an irrigation-stop experiment. *New Phytologist*, *227*, 1081–1096.

- Zweifel, R., & Sterck, F. (2018). A conceptual tree model explaining legacy effects on stem growth. *Frontiers in Forests and Global Change*, *1*(1), 35–115.

SUPPORTING INFORMATION

Additional supporting information can be found online in the Supporting Information section at the end of this article.

How to cite this article: Vitali, V., Schuler, P., Holloway-Phillips, M., D'Odorico, P., Guidi, C., Klesse, S., Lehmann, M. M., Meusburger, K., Schaub, M., Zweifel, R., Gessler, A., & Saurer, M. (2024). Finding balance: Tree-ring isotopes differentiate between acclimation and stress-induced imbalance in a long-term irrigation experiment. *Global Change Biology*, *30*, e17237. <https://doi.org/10.1111/gcb.17237>